Conversion of marginal land into switchgrass conditionally accrues soil carbon and reduces methane consumption

Colin T. Bates,[1,2] Arthur Escalas,[3] Jialiang Kuang[1], Lauren Hale,[4] Yuan Wang,[5] Don Herman,[6,9] Erin E. Nuccio,[6] Xiaoling Wang,[7] Ying Fu,[1,2] Renmao Tian,[1,2] Gangsheng Wang,[1,2] Daliang Ning,[1,2] Yunfeng Yang,[8] Liyou Wu,[1,2] Jennifer Pett-Ridge,[6] Malay Saha,[5] Kelly Craven,[5] Mary Firestone,[10] and Jizhong Zhou[1,2, 8, 10]

[1] The Institute for Environmental Genomics, University of Oklahoma, Norman, OK, USA
[2] Department of Microbiology and Plant Biology, and School of Civil Engineering and Environmental Sciences, University of Oklahoma, Norman, OK, USA
[3] MARBEC, University of Montpellier, Montpellier, France
[4] USDA, Agricultural Research Service, San Joaquin Valley Agricultural Sciences Center, 9611 South Riverbend Avenue, Parlier, CA 93648-9757, USA
[5] Noble Research Institute, Ardmore, OK
[6] Physical and Life Sciences Directorate, Lawrence Livermore National Laboratory, Livermore, CA 94551, USA
[7] The Key Laboratory of Aquatic Biodiversity and Conservation of the Chinese Academy of Sciences; Institute of Hydrobiology, Chinese Academy of Sciences, Wuhan 430072, China
[8] State Key Joint Laboratory of Environment Simulation and Pollution Control, School of Environment, Tsinghua University, Beijing 100084, China
[9] Department of Environmental Science, Policy and Management, University of California, Berkeley, CA 94720, USA
[10] Earth and Environmental Sciences, Lawrence Berkeley National Laboratory, Berkeley, CA 94270, USA

Abstract

Switchgrass (*Panicum virgatum* L.) is a perennial C_4 grass native to tallgrass prairies of the Central US, and a promising bioenergy feedstock. Switchgrass can be cultivated on soils with low nutrient contents and its rooting depth, of up to 2 m, has brought attention to the crop as a potential mechanism to sequester and build soil carbon (C). Switchgrass, therefore, offers multifaceted benefits on degraded soils by enhancing soil organic matter content. However, to evaluate the sustainability of switchgrass-based biofuel production, it is crucial to understand the impacts of land conversion and switchgrass establishment on biotic/abiotic characteristics of

various soils. In this study, we characterized the ecosystem-scale consequences of switchgrass growing at two highly-eroded, 'Dust Bowl' remnant field sites from Oklahoma US, with silt-loam (SL) or clay-loam (CL) soil textures having low nitrogen (N), phosphorus (P), and C contents. Paired plots at each site, including fallow control and switchgrass-cultivated, were assessed. Our results indicated that switchgrass significantly increased soil C at the SL site and reduced microbial diversity at the CL site. The CL site exhibited significantly higher CO_2 flux and higher respiration from switchgrass plots. Strikingly, switchgrass significantly reduced the CH_4 consumption by an estimated 39% for the SL site and 47% for the CL site. Structural equation modeling identified soil temperature, P content, and soil moisture levels as the most influential factors regulating both CO_2 and CH_4 fluxes. CO_2 flux was also influenced by microbial biomass while CH_4 flux was influenced by microbial diversity. Together, our results suggest that site selection by soil type is a crucial factor in improving soil C stocks and mitigating greenhouse gas (GHG) fluxes, especially considering our finding that switchgrass reduced methane consumption, implying that carbon balance considerations should be accounted for to fully evaluate the sustainability of switchgrass cultivation.

Key words: Greenhouse Gases, Carbon Dioxide, Methane, Nitrous Oxide, Switchgrass, Soil Organic Matter, Carbon Sequestration, Biofuel

Introduction

Taking place over three waves during the 1930s, The American 'Dust Bowl' was a catastrophic ecological disaster that brought severe drought and dust storms to the central prairies and affected roughly 40 million hectares of land (Schubert et al., 2004; Worst, 1982; Baumhardt, 2003). Strong wind erosion exacerbated the topsoil displacement, creating many

57 'marginal' lands of low soil nutrient quality across Oklahoma and the Southwestern US (Texas,
58 Kansas, Colorado, and New Mexico). Since then, many of these sites have remained a 'poor' fit
59 for agricultural development. It has been suggested that the implementation of deep-rooted
60 perennial grasses may aid in soil restoration at these sites, offering economic benefits to farmers
61 in the form of cellulosic feedstock for bioenergy production (Gelfand et al., 2013).

62 Switchgrass (*Panicum virgatum* L.), a tall perennial deep-rooted grass native to the Central
63 North American Plains, is an auspicious bioenergy crop suitable for future large-scale cultivation
64 in the US (McLaughlin and Kszos, 2005). This enthusiasm for switchgrass stems from its
65 excellent ability to exhibit high biomass even on low-quality soils unfit for traditional
66 agricultural practices, with little to no additional inputs (Tilman et al., 2006). Long-term
67 cultivation experiments have suggested that switchgrass can improve soil productivity through
68 the net input of soil C (Gelfand et al., 2013, Ma et al., 2000). Therefore, large-scale switchgrass
69 cultivation may offset GHG emissions and serve as a means for improved soil fertility through C
70 sequestration at nutrient-poor sites (Anderson-Teixeria et al., 2009). Switchgrass is also known
71 to be highly drought tolerant (Barney et al., 2009) and can prevent topsoil erosion -two major
72 problems in the Central and Southwestern USA including states of OK, TX, KS, CO, and NM. It
73 is estimated that 15 million hectares of arable land would need to be converted into biofuel crop
74 in order to meet the US Department of Energy's plan to replace 30% of transportation fossil fuels
75 with biofuels by 2030 (Bouton, 2007; Bouton, 2008). An estimated 11% of the contiguous US is
76 considered nutrient-poor or 'marginal' land (Milbrandt et al., 2014) and currently represent an
77 under-utilized resource that may be well suited for switchgrass cultivation (Stoof et al., 2015).
78 Since perennial crop systems have high root biomass and exudates, they can improve soil C
79 stability and aggregate formation (Tiemann and Grandy, 2015). Like other perennial crops,

Switchgrass has been broadly associated with increases in soil C at many different sites in the central and northern Great American Plains (Liebig et at., 2008; Zan et al., 2001; Frank et al., 2004; Dabney et al., 2004). However, this potential C accrual may be offset by higher soil respiration arising from stimulated microbial C mineralization or increased root respiration.

Because soil microorganisms are critical drivers of soil nutrient cycling, understanding plant-microbe interactions during switchgrass cultivation could inform land management strategies toward the promoting of soil nutrient acquisition and recycling, along with reducing GHG emissions. By examining microbial ecology of switchgrass influenced systems, researchers have revealed mechanistic understanding of the ways it enhances ecosystem services such as C sequestration, soil fertility, and GHG emissions (McLaughlin and Kszos, 2005; Ker et al., 2014; Clarck et al., 2005; Bahulikar et al., 2014; Ghirmire et al., 2009; Kim et al., 2012; Ghimire and Craven, 2011). For instance, it was shown that N fertilization, at least at some sites, did not increase soil-surface carbon dioxide (CO_2) emissions despite increases in above (Mulkey et al., 2006; Lee at al., 2007) and below ground biomass (Sher et al., 2020). However, the relative impact of methane (CH_4) emissions during land conversions are not yet fully understood (Monti et al., 2012; Robertson and Grace, 2004; Fritsche et al., 2010). Additionally, the ecological consequences of land conversion, its impact on soil microbial ecology and functionality, as well as the overall sustainability of switchgrass cultivation as a biofuel crop remain to be demonstrated. Further, only a few studies have evaluated switchgrass cultivation at sites with low soil N, C, or P contents or in marginal lands that have experienced high rates of topsoil erosion (Gelfand et al., 2013; Ashiq et al., 2017). Particularly, we currently have a very limited understanding of how the transition from mixed annual grassland communities to switchgrass row-crop systems can affect (i) soil geochemical composition at nutrient-poor sites; (ii) soil

103 microbial biodiversity, and (iii) the overall prairie ecosystem functionality, specifically GHG
104 fluxes.

105 In this study, we monitored the ecosystem-level effects of switchgrass establishment over
106 two consecutive growing seasons (n = 17 months) in two nutrient-poor (relatively low N, P, and
107 C contents) field sites in Southern Oklahoma (designated SL for the silt-loam soil texture and CL
108 for the clay-loam soil texture). We compared switchgrass and natural fallow plots in terms of soil
109 chemistry (C, N, and P), soil GHG fluxes (CO_2, CH_4, and N_2O), and microbial community
110 composition. We tested the hypotheses that annual mixed grassland conversion to switchgrass (i)
111 increases topsoil C levels over time; (ii) switchgrass increases CO_2 respiration while maintaining
112 similar CH_4 emission and N_2O flux relative to annual mixed grassland communities (fallows);
113 and (iii) switchgrass modifies the microbial community during establishment and decreases
114 species richness over time. We expect shifts in microbial community composition to correlate
115 with observed GHG fluxes. Our results indicated that switchgrass had a site-specific, with
116 increased CO_2 respiration and decreases in microbial species richness observed only at the CL
117 site, while soil C accumulation was observed only for the SL site. Switchgrass significantly
118 reduced the methane consumption rates regardless of soil type.

119 # Methods

120 **Field site, soil sampling, and root biomass estimation**

121 Samples were taken from two sites in southern Oklahoma, a silt-loam site (SL) near the
122 Texas border (34.18691°N, -97.08487°W) and a clay-loam site (CL) in Ardmore (34.172100°N,
123 -97.07953°W). Prior to our experiment, each field site had experienced annual crop rotation and
124 periods of being left fallow. At each site, a switchgrass field plot (27 x 22 m) containing 500

genetically distinct individuals of the lowland Alamo variety with a 1 m spacing between plants and a corresponding fallow plot (27 x 22 m) were established in the summer of 2016 (Fig. S1a,b). All plots were tilled before planting switchgrass. Fallow plots were allowed to undergo natural succession of grasses and weeds over the time course of the experiment. To allow GHG measurements, at each plot, 21 PVC collars (diameter 23.63 cm x 12.8 cm x 1 cm) (Fig. S1c) were embedded 8 cm into the soil and placed in a cross design (Fig. S1a,b) with five collars extending in each cardinal direction from a central origin collar at the center of each plot. After trace gas measurement from each collar, two soil cores (15 - 20 cm in depth) were taken from within a 20 cm radius of each collar (Fig. S1d), thoroughly mixed, and separated into two bags, one for geochemical analyses and one for DNA extraction. Sampling flags were placed to prevent re-sampling the same location twice and each core was filled by topsoil taken from outside the plot. All soil samples were immediately stored on ice, transported back to the lab and kept at either 5□ for geochemical analyses or -80□ for DNA extraction. In May 2017, total belowground root biomass was estimated using the Fraiser et al., 2016 method. Briefly, four 0-1 m cores were taken between six target plants and an adjacent plant (Fig. S2b). Soil cores were then divided into 5 depths for every 20 cm of soil. For each depth, roots were extracted from cores through sieving and soaking the soil in water. Roots from each layer of soil were collected, dried and massed from each layer. Switchgrass root biomass was estimated as described elsewhere (Frasier et al., 2016). For fallow plots, four randomly assigned 1 m^2 subplots within each of the quadrants were selected to take four 0-1 m soil cores to represent root biomass across the plot (Fig. S2c). No roots were detected from fallow soil cores below 60 cm depth.

Soil geochemistry, pH, and moisture

Soil pH, moisture, total available C, N, P, nitrate (NO_3), and ammonium (NH_4) were measured following as described elsewhere (Hendershot et al., 2007). Briefly, 10 g of soil was placed into a 50 ml tube with distilled H_2O added to the 50 ml fill line. Tubes were gently shaken for 30 minutes and given an hour to settle before pH measurement using a pH probe (Acccumet excel XL15 pH meter, Fisher Scientific, Hampton NH, USA). Soil moisture was determined by a gravimetric drying protocol that dried > 5 g of soil for one week at > 60 □ before re-massing to establish the percent of water lost after drying. To determine other soil geochemical parameters, soil samples were dried in an oven at 60□ for a week followed by sieving to remove unwanted material with a 4 mm sieve. Soil samples were then shipped seasonally to the Oklahoma State University (OSU) soil testing lab where Mehlich III extractions (to quantify the available P in the soil), KCL extractions (to determine NH_4 and NO_3 concentrations) were performed and total soil C/N amounts were measured via dry combustion (LECO corporation, St. Joseph MI, USA).

Environmental parameters

Daily environmental data for 21 different environmental variables (at 5 to 15-minute resolution) were obtained from two weather monitoring stations (Ardmore and Burneyville) belonging to the Oklahoma MESONET network (http://mesonet.org/) that were the closest to our field sites (1.43 km and 2.3 km from SL and CL, respectively). Variables used included air temperature, bare soil temperature, covered soil temperature, atmospheric pressure, relative humidity, and precipitation (Table S1 and Table S2).

Trace gas fluxes

The CO_2, CH_4, and N_2O fluxes were measured monthly via cavity ring-down spectrometry using a Picarro G2508 analyzer (Picarro, Santa Clara, CA, U.S.A.). Measurements

were taken continuously every 2 seconds from a total of 6 minutes per collar. This allowed us to obtain gas concentrations in parts per million. Raw data from each gas were separated and then manually inspected to remove the beginning and the end of the measurements, which are often influenced by the pushing/pulling of the gas chamber. Then three models (linear, quadratic, and exponential) were fitted for each sample and gas species to characterize the variation of gas concentrations across time and the 'best model' was selected based on AIC scores. Flux estimations for each of the gases were then calculated using the following equation (Christiansen et al., 2015):

$$F = \frac{dC}{dt} \cdot \frac{PV}{A \cdot R(273.15+T)} \times 3600$$

Where $\frac{dC}{dt}$ is the slope of the best fitted model at t = 0, V is the chamber volume (L), A is the chamber area (m^2), R is the gas constant in L atm K^{-1} mol^{-1}, T is the temperature in Celsius, when the chamber pressure is assumed to be equal to 1 atm. The 3600 factor is included to convert the flux to hourly values. For CO_2 flux, F was then divided by 1000 to obtain the correct units of millimoles per m^2 per hour.

Soil DNA extractions, microbial community sequencing and analysis

A freeze grinding method (Zhou et al., 1996) was combined with the Powersoil DNA extraction kit (Qiagen, Venlo, Netherlands) to extract DNA from a total of 1,428 soil samples, which typically yielded soil DNA of both high quantity and quality. For microbial community profiling a two-step PCR method (Wu et al., 2015) was used for amplification of the V4 region of the bacterial 16S rRNA gene using the 515F, 5'-GTGCCAGCMGCCGCGGTAA-3' and 806R, 5'-GGACTACHVGGGTWTCTAAT-3' primers. Sequencing of the 16S rRNA gene

amplicons was conducted on the Illumina Mi-Seq DNA sequencing platform (Illumina Inc., San Diego, CA, U.S.A.). Amplicon sequence data was analyzed using an internal pipeline known as the Amplicon Sequencing Analysis Pipeline (Zhang et al., 2014) (ASAP, version 1.4). MiSeq sequences were quality checked with FastQC (version 0.11.5), pair-end sequences were merged based on their 3' overlap using PEAR (version 0.9.10) with a quality score cutoff set to 20, and assembly length between 200-400 with the minimum overlap length set to 50 bp. The program *split_libraries_fastq.py* from the QIIME package (Kuczynski et al., 2012) (version 1.9.1) was used to assign reads to each sample (demultiplexing) based on the barcodes for each individual sample with a maximum allowed barcode error of 0 and the trimming quality score set to 20. Primer sequences were then trimmed and removed. Sequences from multiple split libraries were merged together. Dereplication was performed by USEARCH (Edgar, 2010) (version 9.2.64) using the command *fastx_uniques* (utilizing the size-out option for sequence abundance output). Operational Taxonomic Units (OTUs) were clustered using UPARSE, with the OTU identity threshold set to 0.97 and the singletons/chimeric sequences removed (Edgar, 2013). The OTU table was generated by the command *-usearch_global* in USEARCH. Each representative sequence for each OTU was classified with the RDP Classifier (Wang et al., 2007) (16S: training set 16, June 2016) with the confidence cutoff set to 0.8. OTUs in the 16S sequence reads assigned to Chloroplast at the Order level were removed. Representative sequences for each OTU were used to construct a phylogenetic tree. Sequences were then aligned using MAFFT (Katoh, 2002) (version 3.8.31) and alignments were filtered using Gblocks (Castresana, 2000) (version 0.91b) with the options -t=d, -b4=3 and -b5=h. FastTree (Price et al., 2009) was used for constructing the phylogenetic tree using the filtered alignments. The phylogenetic tree and OTU

tables were used to calculate alpha diversity (phylogenetic based indexes) and beta diversity (UniFrac distance) using programs packaged in QIIME (Caporaso et al., 2010) and R.

Statistical analyses

All analyses were conducted using R statistical software (3.4.4, R Core Team, 2014) and figures were produced using the package ggplot2 (Wickham, 2009). Data normality was tested using the Shapiro test. We tested for differences between plots in GHG flux and microbial alpha diversity by using linear mixed models to correct for repeated measurements (i.e. collars within plots) and to analyze the data over time (R package *lme4*, Bates et al., 2015). Pairwise comparisons for soil respiration between treatments were conducted using Wilcoxon Rank Sum test and effect sizes were calculated using Mann-Whitney U Test. Differences in soil biogeochemical properties between treatment were tested using Kruskal-Wallis test and effect size was calculated using epsilon squared. Soil geochemical dissimilarity was calculated from scaled data using Euclidean distances (*vegan* R package). Then mean dissimilarity across collars was used to construct linear mixed models to view changes in dissimilarity over time. Differences in microbial community structure across plot, site and time were tested using PERMANOVA test based on Bray Curtis and weighted-UniFrac dissimilarity for taxonomic and phylogenetic diversity, respectively. Differences in relative abundance between groups and time points was calculated by multiple Student T-Tests and p-values were adjusted by conservative Bonferroni correction to compensate for increased Type 1 errors over multiple time points.

Structural equation modeling **(**SEM) were used to explore the direct and indirect relationships among environmental variables and GHG fluxes (CO_2 and CH_4) at either site. We first considered a full model that included all reasonable pathways, then eliminated nonsignificant pathways until we obtained a final model with only significant pathways. We used

a χ^2 test and the root mean square error (RMSE) to evaluate the fit of our model. The SEM-related analysis was performed using the lavaan R package (Rosseel, 2012).

Results

Changes in soil geochemistry

The conversion of grassland into switchgrass appeared to have a site-specific impact on soil geochemistry. A principal component analysis (PCA) of the soil geochemistry data revealed strong differences between the two sites (Figure 1). Heterogeneity of the geochemical parameters was higher at the CL site, as displayed by the dispersion of blue samples in Figure 1.

The total soil C at the SL site increased over the 17-month period in the switchgrass plot (Figure 2a) (r^2 = 0.12, $p < 0.001$) and was significantly higher than the fallow (Table 1, $p < 0.001$, large effect size = 0.4). Switchgrass also had a homogenizing effect for soil C, reducing the overall dissimilarity between samples compared to the fallow plots, which had patchy plant cover. These increases in soil C were occurring evenly across the plots area (Fig. S3a). In contrast, the total soil C content remained constant in the CL switchgrass plot (Figure 2a).

Total soil N was significantly higher in the switchgrass plot at SL compared to the fallow plot (Table 1, $p < 0.0001$, medium effect size = 0.19) and these N levels significantly decreased over time (r^2 = 0.05, $p < 0.01$) (Figure 2b), coinciding with an increase in the soil N heterogeneity in the plot (r^2 = 0.12, $p < 0.0001$) (Fig. S3b). A significant increase in the total soil N was notable in the CL fallow plot (r^2 = 0.12, $p < 0.01$) (Figure 2b). Nitrate concentration was significantly reduced for the switchgrass treatment at the SL site (Table 1, $p < 0.001$, small effect size = 0.06). All sites and plots showed a significant reduction in NO_3 concentrations over time

(Fig. S4) despite an increasing homogeneity (Fig. S3). No significant differences or trends were observed in NH_4 concentrations during the length of our study at either site (Fig. S3e and S4b).

Total plant available P levels decreased over time in the SL site ($r^2 = 0.05$, $p < 0.01$) (Figure 2c) and the P content homogenized across the plot (Fig. S3c) despite the SL switchgrass treatment having significantly higher total plant available P content compared to the fallow (Table 1, $p < 0.0001$, large effect size = 0.44). In the CL site, plant available P also decreased in the switchgrass plot compared to the fallow (Table 1, $p < 0.001$, medium effect size = 0.095, and Figure 2c).

Differences in estimated root biomass

Field-scale estimates of belowground root biomass (Fig. S2a) showed a large difference in the root biomass between each switchgrass plot and the corresponding fallow (17.8 and 64 times higher for SL and CL, respectively). Root biomass was estimated for each soil layer in kilograms per meter squared and compared to switchgrass estimates. Estimated total root biomass of the switchgrass plots was 16.9 kg/m^2 for the SL site and 14.1 kg/m^2 for the CL site, while the fallows were 0.95 kg/m^2 for SL and 0.22 kg/m^2 for CL. Generally, root biomass decreased along the soil depth profile for both sites. SL switchgrass site had increased root biomass estimates at lower depths (60-100 cm) than the CL site, which contributed to a slightly higher total root biomass.

Greenhouse gas (GHG) fluxes at the soil-atmosphere interface

CO_2 flux at both sites exhibited a similar seasonal trend with the apex of emissions occurring during summer months and the minimum in late Fall/early Winter months. At the SL site, switchgrass treatment led to significantly higher total CO_2 flux for 29% of the months after

switchgrass planting (Wilcoxon $p < 0.001$, Figure 3a) while the fallow was significantly higher for only 24% of the total months measured. The average CO_2 flux over the 17-months did not differ in the SL site between switchgrass (6.76 ± 5.23 millimoles·m^2·$hour^{-1}$) and the fallow (6.87 ± 5.87 millimoles·m^2·$hour^{-1}$) (Figure 3d). At the CL site, there was a significant difference between treatments (Figure 3d) in the average CO_2 flux over the 17-month period ($p < 0.001$) with the switchgrass plot at 9.98 ± 6.04 millimoles·m^2·$hour^{-1}$ and the fallow at 9.22 ± 6.62 millimoles·m^2·$hour^{-1}$, although the effect size was small (0.13). When comparing the two sites, CL exhibited significantly higher total soil CO_2 fluxes for both switchgrass and fallow plots than those measured at SL (Wilcoxon $p < 0.001$).

CH_4 flux (Figure 3b, Table S3) differed significantly between switchgrass and fallow (Wilcoxon $p < 0.001$, small effect size = 0.15), with a tendency toward higher CH_4 emissions or lower CH_4 consumption levels in the switchgrass plot observed for 41% of the months (Figure 3b) after switchgrass was planted (41% and 52% for CL and SL, respectively). CH_4 flux in the fallow was higher only at one time point (14^{th} month after switchgrass establishment). Overall, the 17-month average CH_4 consumption rate was -0.44 ± 1.07 micromoles·m^2·$hour^{-1}$ for switchgrass treatments (-0.46 ± 1.08 and -0.41 ± 1.06 micromoles·m^2·$hour^{-1}$ for CL and SL, respectively) while it reached -0.77 ± 1.15 in the fallow (-0.76 ± 1.78 and -0.77 ± 0.53 and micromoles·m^2·$hour^{-1}$ for CL and SL, respectively) (Figure 3e, Table S3). Together, a significant ($p < 0.05$, a small effect size = 0.14) switchgrass treatment effect on reducing CH_4 consumption rates was observed at both sites. No significant differences were found for N_2O flux between the switchgrass (-0.26 ± 2.55 micromoles·m^2·$hour^{-1}$ at CL and -2.88 ± 2.09 micromoles·m^2·$hour^{-1}$ at SL) and fallow plots (-1.65 ± 2.5 micromoles per m^2 per hour at CL and -5.01 ± 2.16 micromoles

per m^2 per hour at SL) at either site (Figure 3c, Table S3) over the 17-months of observations (Figure 3f).

Microbial community dynamics

Microbial alpha diversity, calculated as the OTU richness, responded in a site-specific manner to switchgrass cultivation. In the SL site, OTU richness was significantly higher in the switchgrass plot (Table S3, $p < 0.0001$, Medium effect size = 0.38). OTU richness did not change over time in the SL switchgrass plot (Figure 4a) but increased in the fallow plot ($p < 0.001$), despite a decrease in phylogenetic diversity (PD) ($p < 0.05$, Figure 4a,b). At the CL site, species richness decreased significantly over time in both switchgrass ($p < 0.01$) and fallow plots ($p < 0.001$). For PD, this decay was observed only in the switchgrass plot ($p < 0.01$). Chao1 and Shannon index showed similar trends per site over time (Fig. S5).

We observed significant differences in the bacterial community structure (beta diversity) between sites, plant cover type, and over time (Figure 4c, PERMANOVA, $p < 0.01$, Table S4). Relative abundance of major phyla showed large changes from the initial planting/before soil tillage and two months after the experiment began (Figure 5). At all sites, at least five abundant phyla exhibited changes in relative abundance. Firmicutes phyla relative abundance (0.6 – 0.14 %) changed over the course of the experiment in both fallow plots. The structure of microbial communities from the switchgrass plots appeared less variable than their corresponding fallows. In the CL site, the strongest differences in dominant phyla relative abundance between plots (switchgrass vs fallow) were observed at eight and fourteen months after switchgrass planting (Feb. 2017 and Aug. 2017, Table S5). After eight months, seven phyla (Actinobacteria, Bacteroidetes, Chloroflexi, Deinococcus-Thermus, Firmicutes, Plactomycetes, and Verrucomicrobia) exhibited different abundance between treatment, while only four phyla

(Actinobacteria, Chloroflexi, Cyanobacteria, and Deinococcus-Thermus) were different after fourteen months. For the SL site, the largest shifts in community composition occurred in the last two time points, *i.e*. fourteen and sixteen months after switchgrass establishment. After fourteen months, three phyla were significantly different between treatment (Acidobacteria, Bacteroidetes and Deinococcus-Thermus) and after sixteen months four groups were significantly different (Acidobacteria, Bacteroidetes, Cyanobacteria, and Verrucomicrobia).

Canonical correspondence analysis (CCA) was used to link environmental variables to the microbial community (Figure 6). A clear separation between microbial communities from the two sites was observed. Microbial communities from the SL site were correlated with plant available P and soil pH, while CL communities were associated with total soil N, NH_4, and NO_3. In addition, fallow communities from CL were dispersed, while switchgrass communities at this site were clustered by N source or along a soil moisture profile.

Structural equation model

Structural equation modeling (SEM) was used for an in-depth analysis of the direct and indirect effects of the environmental drivers on CO_2 and CH_4 flux for both sites. Correlations between all variables are shown in the correlogram Figure S6. For CO_2 fluxes (Figure 7a) the model confirmed the importance of the site effect on soil geochemistry and microbial communities, with the strongest direct effects (based on standardized coefficient) being directed from the site towards total C ($\beta = -0.95$, $p < 0.001$), total N ($\beta = -0.94$, $p < 0.001$), P levels ($\beta = 0.88$, $p < 0.001$), and microbial alpha diversity ($\beta = 0.52$, $p < 0.001$). Plant available P tended to influence the levels of C and N in the system, and these three components of soil have significant effects on CO_2 fluxes. Other important variables influencing CO_2 fluxes included soil temperature ($\beta = 0.69$, $p < 0.001$), moisture ($\beta = 0.27$, $p < 0.001$) and microbial biomass ($\beta =$ -

346 0.18, $p < 0.001$). This later variable appeared mostly dependent on N content ($\beta = 0.56$, $p <$
347 0.001).

348 In the CH_4 model (Figure 7b), which was focused on the switchgrass plots, the site effect
349 appeared less pronounced and mostly directed toward P levels ($\beta = -0.29$, $p < 0.001$) and
350 microbial alpha diversity ($\beta = 0.62$, $p < 0.001$). Although soil temperature did not have a very
351 strong influence on CH_4 fluxes ($\beta = -0.19$, $p < 0.001$), it was still important in this model through
352 many direct effects on P ($\beta = 0.07$, $p < 0.001$), NO_3 ($\beta = 0.23$, $p < 0.001$), pH ($\beta = -0.22$, $p <$
353 0.001), microbial diversity ($\beta = 0.11$, $p < 0.001$), and moisture ($\beta = -0.39$, $p < 0.001$). Overall, we
354 were able to show that CH_4 fluxes depended on a combination of soil chemical properties (P and
355 NO_3) along with physical (temperature and moisture) and biological (microbial diversity)
356 characteristics.

357 # Discussion

358 Our study illustrates that soil type is a key component of switchgrass' ability to improve soil
359 quality and appears crucial for its use as a sustainable bioenergy feedstock. It was hypothesized
360 that switchgrass would increase (i) topsoil C levels and (ii) increased CO_2 respiration -with (iii)
361 little effect on CH_4 emissions and N_2O flux, but also (iv) decreased the bulk soil microbial
362 species richness relative to annual mixed grassland communities. While C accrual, CO_2
363 respiration, and microbial richness reductions were site-dependent in our study, switchgrass
364 significantly altered the soil CH_4 sink capacity at both sites by reducing the overall CH_4
365 consumption rates. Although the CH_4 emission rates reported here were expectedly lower than
366 those reported for natural systems with anaerobic, water-logged conditions like peatlands (Dise,
367 1993) and wetlands (Bridgham et al., 2013; Bartlett and Harriss, 1993), our findings challenged

368 the notion that CH_4 emissions has negligible effects on GHG budgets during marginal land
369 transitions to switchgrass row-cropping (Monti et al., 2012). However, comprehensive GHG
370 budgets along with spatial-explicit modeling of soil and plant C stocks should be considered to
371 fully evaluate the net effect of land type conversion at these prairie sites.

372 **Soil type dictates the effects that switchgrass has on geochemistry**

373 Our study revealed significant site-level differences to switchgrass establishment on soil C
374 accrual, total soil N levels and depletion of soil P content. The CL site with higher relative
375 nutrient content showed little change over time (17 months) for any of the soil geochemical
376 parameters. Ma et al., 2000 reported changes in soil geochemistry by switchgrass cultivation in
377 clay-loam soils were only detected after longer periods of time (over a decade). Therefore,
378 prolonged sampling at our CL site will improve assessments of switchgrass-induced soil C
379 changes. Nitrate contents (Figure S4a) significantly declined with time, which may suggest
380 assimilation by the switchgrass or an increased activity of denitrifying bacteria. It is also notable
381 that the crop was grown under natural conditions without applying any chemical fertilizers.

382 The SL site showed significant increases in soil C content for the top-soil layer (27% higher
383 total C after two growing seasons) over the course of switchgrass establishment. This is
384 consistent with estimates of switchgrass systems repaying their C debt in a relatively short
385 amount of time (Abrah et al., 2019). However, switchgrass led to significant depletions in soil N
386 and P contents at the SL site over time, though these values were higher than the fallow from the
387 beginning of our experiment. One explanation for this observation is the increased below ground
388 root biomass estimates being larger for the SL site at lower depths. Greater investment of
389 belowground root biomass may reflect the higher plant available P conditions at this site,

allowing switchgrass to extend deeper into the subsurface soil for water or micronutrient availability.

Seasonal sampling of NH_4-N sources was not sufficient in explaining large seasonal variations observed over the time course of our experiment. For example, a spike in soil NH_4 levels (Figure S4b) was detected during October of 2016 and June of 2017, which could be the signature of episodic N fixation events occurring in switchgrass during/before flowering as reported previously (Roley et al., 2019). However, our resolution in sampling this geochemical parameter is not sizeable enough to adequately explain these anomalies.

Microbial community shifts under switchgrass establishment

Microbial community diversity and composition at each site had differential responses to switchgrass establishment. Broadly, alpha diversity measures in CL decreased over time and revealed a higher amount of clustering and similarity in the overall community structure compared with the fallow. Analogous to secondary plant successional dynamics, the microbial community at the CL site may be more influenced by the change from short rooted annuals to the monoculture of deep-rooted perennial switchgrass, causing a loss in microbial diversity (Cline and Zak, 2015). For SL, switchgrass cultivation significantly increased the Shannon index over time and caused the community composition to shift away from the fallow. This may be indicative of the improvements of soil quality, which changed the functionality of the microbial community due to the influence of switchgrass on increases in soil C levels (Leff et al., 2015).

Microbial community structure was altered by switchgrass establishment (Table S4) and through time at each of the sites relative to the fallow soil communities. These changes in community structure may reflect different survival strategies that switchgrass may employ in the

412 recruitment of specific taxa to its rhizosphere based of differences between the geochemistry of
413 the two sites. Investigations into rhizosphere microbiome succession during establishment may
414 provide insights into direct plant-microbe interactions that facilitate switchgrass establishment in
415 these nutrient-poor soils.

416 **Factors controlling soil GHG flux**

417 Contrary to our hypothesis, CO_2 respiration was significantly enhanced by switchgrass
418 establishment only at the CL site. We expected higher root respiration and the potential for deep
419 C mineralization to enhance soil respiration at both sites after switchgrass establishment
420 (Shahzad et al., 2018; Fontaine et al., 2007). The CL site had an overall higher total CO_2
421 emission rate during our field monitoring. This response may be mediated by the relatively
422 higher preexisting C nutrient conditions found at this clay-loam site (Kang et al., 2016) as root
423 biomass levels were estimated to be similar at each site. This illustrates a benefit in site selection
424 by soil type in minimizing CO_2 released during land conversion.

425 Nitrous oxide fluxes did not show any significant effect between either site or plant cover
426 type. Thus, we did not see an effect of switchgrass or site on nitrous oxide fluxes. However,
427 nitrous oxide fluxes were marked by high variability, both seasonally and spatially within each
428 plot. Efforts were made to correlate rainfall events to reduce noise in the flux signal, but a
429 substantial limitation was our six-minute window of continuous measurements per sampling
430 event. A longer period of trace gas sampling may have resulted in a more stable signal with less
431 variability for nitrous oxide fluxes.

432 Methane flux monitoring showed a significant reduction in CH_4 consumptions at both
433 sites with switchgrass introduction and cultivation. Although CH_4 emission rates were low and

434 measured at only a few time points, consistently lower CH_4 consumption rates were observed
435 throughout the monitoring period of our experiment. Total methane consumption rates for
436 switchgrass plots were reduced by 47% and 39% compared to corresponding fallow sites for CL
437 and SL, respectively. This could reflect considerable differences in the net C budget and fluxes
438 for these switchgrass sites. In the future, GeoChip-based functional microarray (Shi et al., 2019)
439 as well as, RT-qPCR of CH_4 monooxygenase and methyl-coenzyme M reductase genes may help
440 provide us with specific linkages between microbial functionality potential and our reported CH_4
441 emissions at key time points during our experimental monitoring.

442 # Conclusion

443 Overall, soil C levels increased by 27% during the 17 months experiment in the site with the
444 lowest nutrient content (silt loam, SL) while they remained consistent in the clay loam (CL) site.
445 Switchgrass significantly affected total CO_2 respiration at the CL site, but not at the SL site
446 compared to the annual mixed grassland community fallows and showed a difference in the site
447 level emissions. Grassland conversion to switchgrass reduced the annual CH_4 consumption by 39
448 to 47%, implying that methane fluxes should be accounted for in C budgets to reach a
449 sustainable cultivation of switchgrass. Switchgrass establishment had a significant influence on
450 the microbial community composition over time. Our SEM analysis indicated that soil
451 temperature and moisture were strong environmental drivers of the soil the CO_2 and CH_4 flux at
452 each site. Considerations on soil type and nutrient conditions should be made for the selection of
453 future sites suitable for large-scale bioenergy cultivation of that meets objectives for terrestrial C
454 sequestration and improved soil fertility.

455

Acknowledgements

We would like to thank the Oklahoma Mesonet environmental monitoring network, and particularly Bradley Ilston, for the use of their weather monitoring stations for this work. We deeply appreciate all the help from the auxiliary staff and field hands from the Nobel Research Institute, who aided in us in collecting data and maintaining the field sites for this project. A. Escalas and C. Bates would like to give a special thanks to Randy Freeman, who helped a lot for making sample collection and processing possible. We would also like to thank the following for their contributions in field sampling and molecular work: Zhigang Wang, Yuguang Zhang, Ning Hu, Yan He, Zhongfang Li, Qian Li, Jinyu Hou, Xiubin Ke, Juan Ling, Zheng Gao, and Daniel Curtis. C. Bates would also like to thank Cheryl Bates for edits and Tanya Ball for support during this project. This research is supported by the U.S. Department of Energy Office of Science, Office of Biological and Environmental Research Genomic Science program under the award number DE-SC0014079 to the UC Berkeley, Nobel Research Institute, University of Oklahoma, the Lawrence Livermore National Laboratory, and the Lawrence Berkeley National Laboratory.

References

1. Abraha M, Gelfand I, Hamilton SK, Chen J, Robertson GP. Carbon debt of field-scale conservation reserve program grasslands converted to annual and perennial bioenergy crops. Environ Res Lett. 2019;
2. Anderson-Teixeria KJ, Davis SC, Masters MD, Delucia EH. Changes in soil organic carbon under biofuel crops. GCB Bioenergy. 2009;
3. Ashiq MW, Bazrgar AB, Fei H, Coleman B, Vessey K, Gordon A, et al. A nutrient-based sustainability assessment of purpose-grown poplar and switchgrass biomass production systems established on marginal lands in Canada. Can J Plant Sci. 2017;
4. Bahulikar RA, Torres-Jerez I, Worley E, Craven K, Udvardi MK. Diversity of nitrogen-fixing bacteria associated with switchgrass in the native tallgrass prairie of Northern Oklahoma. Appl Environ Microbiol. 2014;
5. Barney JN, Mann JJ, Kyser GB, Blumwald E, Van Deynze A, DiTomaso JM. Tolerance of switchgrass to extreme soil moisture stress: Ecological implications. Plant Sci. 2009;
6. Bartlett KB, Harriss RC. Review and assessment of methane emissions from wetlands. Chemosphere. 1993;
7. Bates D, Mächler M, Bolker BM, Walker SC. Fitting linear mixed-effects models using lme4. J Stat Softw. 2015;
8. Baumhardt LR. Dust Bowl Era. In: Encyclopedia of Water Science. 2003.
9. Bouton JH. Molecular breeding of switchgrass for use as a biofuel crop. Current Opinion in Genetics and Development. 2007;
10. Bouton, J. in *Genetic Improvement of Bioenergy Crops* (ed W. Vermerris) 295-308 Springer Science and Business Media, 2008;

11. Bridgham SD, Cadillo-Quiroz H, Keller JK, Zhuang Q. Methane emissions from wetlands: Biogeochemical, microbial, and modeling perspectives from local to global scales. Glob Chang Biol. 2013;
12. Caporaso JG, Kuczynski J, Stombaugh J, Bittinger K, Bushman FD, Costello EK, et al. QIIME allows analysis of high-throughput community sequencing data. Nature Methods. 2010;
13. Castresana J. Selection of conserved blocks from multiple alignments for their use in phylogenetic analysis. Mol Biol Evol. 2000;
14. Christiansen JR, Outhwaite J, Smukler SM. Comparison of CO2, CH4 and N2O soil-atmosphere exchange measured in static chambers with cavity ring-down spectroscopy and gas chromatography. Agric For Meteorol. 2015;
15. Clark RB, Baligar VC, Zobel RW. Response of mycorrhizal switchgrass to phosphorus fractions in acidic soil. Commun Soil Sci Plant Anal. 2005;
16. Cline LC, Zak DR. Soil microbial communities are shaped by plant-driven changes in resource availability during secondary succession. Ecology. 2015;
17. Dabney SM, Shields FD, Temple DM, Langendoen EJ. Erosion processes in gullies modified by establishing grass hedges. Trans Am Soc Agric Eng. 2004;
18. Dise NB. Methane emission from Minnesota peatlands: Spatial and seasonal variability. Global Biogeochem Cycles. 1993;
19. Edgar RC. Search and clustering orders of magnitude faster than BLAST. Bioinformatics. 2010;
20. Edgar RC. UPARSE: Highly accurate OTU sequences from microbial amplicon reads. Nat Methods. 2013;

519 21. Fontaine S, Barot S, Barré P, Bdioui N, Mary B, Rumpel C. Stability of organic carbon in
520 deep soil layers controlled by fresh carbon supply. Nature. 2007;
521 22. Frank AB, Berdahl JD, Hanson JD, Liebig MA, Johnson HA. Biomass and carbon
522 partitioning in switchgrass. Crop Sci. 2004;
523 23. Frasier I, Noellemeyer E, Fernández R, Quiroga A. Direct field method for root biomass
524 quantification in agroecosystems. MethodsX. 2016;
525 24. Fritsche UR, Sims REH, Monti A. Direct and indirect land-use competition issues for
526 energy crops and their sustainable production - an overview. Biofuels, Bioproducts and
527 Biorefining. 2010;
528 25. Gelfand I, Sahajpal R, Zhang X, Izaurralde RC, Gross KL, Robertson GP. Sustainable
529 bioenergy production from marginal lands in the US Midwest. Nature. 2013;
530 26. Ghimire SR, Charlton ND, Craven KD. The mycorrhizal fungus, sebacina vermifera,
531 enhances seed germination and biomass production in switchgrass (panicum virgatum l).
532 Bioenergy Res. 2009;
533 27. Ghimire SR, Craven KD. Enhancement of Switchgrass (Panicum virgatum L.) Biomass
534 Production under Drought Conditions by the Ectomycorrhizal Fungus Sebacina
535 vermifera. Appl Environ Microbiol. 2011;
536 28. Hartman JC, Nippert JB, Orozco RA, Springer CJ. Potential ecological impacts of
537 switchgrass (Panicum virgatum L.) biofuel cultivation in the Central Great Plains, USA.
538 Biomass and Bioenergy. 2011;
539 29. Hendershot W, Lalande H, Duquette M. Soil Reaction and Exchangeable Acidity. In: Soil
540 Sampling and Methods of Analysis, Second Edition. 2007;

30. Jobbágy EG, Jackson RB. The distribution of soil nutrients with depth: Global patterns and the imprint of plants. Biogeochemistry. 2001;
31. Kang H, Fahey TJ, Bae K, Fisk M, Sherman RE, Yanai RD, et al. Response of forest soil respiration to nutrient addition depends on site fertility. Biogeochemistry. 2016;
32. Katoh K. MAFFT: a novel method for rapid multiple sequence alignment based on fast Fourier transform. Nucleic Acids Res. 2002;
33. Ker K, Seguin P, Driscoll BT, Fyles JW, Smith DL. Evidence for enhanced N availability during switchgrass establishment and seeding year production following inoculation with rhizosphere endophytes. Arch Agron Soil Sci. 2014;
34. Kim S, Lowman S, Hou G, Nowak J, Flinn B, Mei C. Growth promotion and colonization of switchgrass (Panicum virgatum) cv. alamo by bacterial endophyte burkholderia phytofirmans strain PsJN. Biotechnol Biofuels. 2012;
35. Kuczynski J, Stombaugh J, Walters WA, González A, Caporaso JG, Knight R. Using QIIME to analyze 16s rRNA gene sequences from microbial communities. Curr Protoc Microbiol. 2012;
36. Lee DK, Doolittle JJ, Owens VN. Soil carbon dioxide fluxes in established switchgrass land managed for biomass production. Soil Biol Biochem. 2007;
37. Leff JW, Jones SE, Prober SM, Barberán A, Borer ET, Firn JL, et al. Consistent responses of soil microbial communities to elevated nutrient inputs in grasslands across the globe. Proc Natl Acad Sci U S A. 2015;
38. Liang C, Jesus E da C, Duncan DS, Quensen JF, Jackson RD, Balser TC, et al. Switchgrass rhizospheres stimulate microbial biomass but deplete microbial necromass in agricultural soils of the upper Midwest, USA. Soil Biol Biochem. 2016;

564 39. Liebig MA, Schmer MR, Vogel KP, Mitchell RB. Soil Carbon Storage by Switchgrass
565 Grown for Bioenergy. BioEnergy Res. 2008;
566 40. Ma Z, Wood CW, Bransby DI. Soil management impacts on soil carbon sequestration by
567 switchgrass. Biomass and Bioenergy. 2000;
568 41. McLaughlin SB, Kszos LA. Development of switchgrass (Panicum virgatum) as a
569 bioenergy feedstock in the United States. Biomass and Bioenergy. 2005;
570 42. Milbrandt AR, Heimiller DM, Perry AD, Field CB. Renewable energy potential on
571 marginal lands in the United States. Renewable and Sustainable Energy Reviews. 2014;
572 43. Monti A, Barbanti L, Zatta A, Zegada-Lizarazu W. The contribution of switchgrass in
573 reducing GHG emissions. GCB Bioenergy. 2012.
574 44. Mulkey VR, Owens VN, Lee DK. Management of switchgrass-dominated conservation
575 reserve program lands for biomass production in South Dakota. Crop Sci. 2006;
576 45. Price MN, Dehal PS, Arkin AP. Fasttree: Computing large minimum evolution trees with
577 profiles instead of a distance matrix. Mol Biol Evol. 2009;
578 46. Robertson GP, Grace PR. Greenhouse gas fluxes in tropical and temperate agriculture:
579 The need for a full-cost accounting of global warming potentials. Environ Dev Sustain.
580 2004;
581 47. R Core Team. R Core Team (2014). R: A language and environment for statistical
582 computing. R Found Stat Comput Vienna, Austria URL http//wwwR-project.org/. 2014;
583 48. Roley SS, Xue C, Hamilton SK, Tiedje JM, Robertson GP. Isotopic evidence for episodic
584 nitrogen fixation in switchgrass (Panicum virgatum L.). Soil Biol Biochem. 2019;
585 49. Rosseel Y. Lavaan: An R package for structural equation modeling. J Stat Softw. 2012;

50. Schubert SD, Suarez MJ, Pegion PJ, Koster RD, Bacmeister JT. On the Cause of the 1930s Dust Bowl. Science (80-). 2004;

51. Shahzad T, Rashid MI, Maire V, Barot S, Perveen N, Alvarez G, et al. Root penetration in deep soil layers stimulates mineralization of millennia-old organic carbon. Soil Biol Biochem. 2018;

52. Sher Y, Baker NR, Herman D, Fossum C, Hale L, Zhang X, et al. Microbial extracellular polysaccharide production and aggregate stability controlled by switchgrass (Panicum virgatum) root biomass and soil water potential. Soil Biol Biochem. 2020;

53. Shi Z, Yin H, Van Nostrand JD, Voordeckers JW, Tu Q, Deng Y, et al. Functional Gene Array-Based Ultrasensitive and Quantitative Detection of Microbial Populations in Complex Communities. mSystems. 2019;

54. Stoof CR, Richards BK, Woodbury PB, Fabio ES, Brumbach AR, Cherney J, et al. Untapped Potential: Opportunities and Challenges for Sustainable Bioenergy Production from Marginal Lands in the Northeast USA. Bioenergy Research. 2015;

55. Tiemann LK, Grandy AS. Mechanisms of soil carbon accrual and storage in bioenergy cropping systems. GCB Bioenergy. 2015;

56. Tilman D, Hill J, Lehman C. Carbon-negative biofuels from low-input high-diversity grassland biomass. Science (80-). 2006;

57. Wang Q, Garrity GM, Tiedje JM, Cole JR. Naïve Bayesian classifier for rapid assignment of rRNA sequences into the new bacterial taxonomy. Appl Environ Microbiol. 2007;

58. Wickham H. ggplot2: elegant graphics for data analysis. Springer New York. 2009;

59. Worster D. Dust bowl: the Southern Plains in the 1930s (Oklahoma and Kansas). Dust bowl South Plains 1930s (Oklahoma Kansas). 1982;

60. Wu L, Wen C, Qin Y, Yin H, Tu Q, Van Nostrand JD, et al. Phasing amplicon sequencing on Illumina Miseq for robust environmental microbial community analysis. BMC Microbiol. 2015;

61. Zan CS, Fyles JW, Girouard P, Samson RA. Carbon sequestration in perennial bioenergy, annual corn and uncultivated systems in southern Quebec. Agric Ecosyst Environ. 2001;

62. Zhang J, Kobert K, Flouri T, Stamatakis A. PEAR: A fast and accurate Illumina Paired-End reAd mergeR. Bioinformatics. 2014;

63. Zhou J, Bruns MA, Tiedje JM. DNA recovery from soils of diverse composition. Appl Environ Microbiol. 1996;

Table and Figure Captions

Table 1: Differences in physico-chemical soil properties for each site and treatment after 17-months. Values are mean ± SD values and significance was tested by Kruskal-Wallis rank sum test.

Figure 1. **Differences in soil geochemical properties between the two studied sites**. Principal component analysis. Blue colors represent the CL site while red/orange colors signify the SL site. Dark colors represent the SG samples. Variation contained in each PC axis are displayed next to each axis.

Figure 2. **Changes in soil chemistry through two seasons of switchgrass establishment. a**, Total soil carbon percentages; **b**, Total soil nitrogen percentages; **c**,

630 Concentration of plant available phosphate content in parts per million. The best linear
631 model describing the relationship is presented. W_s: estimated model slope and associated
632 error. p-values represent the significance of each model. Each time point is comprised of
633 twenty-one replicates per plot.

634 **Figure 3. Greenhouse gas (GHG) fluxes during grassland conversion to switchgrass.**
635 **a**, **b**, **c**: GHG fluxes at each site over 17 months (mean and standard error estimated using
636 21 replicates for each time points) for: **a**, carbon dioxide flux; **b**, methane flux; **c**, nitrous
637 oxide. **d**, Average GHG fluxes over 17-months for: **d**, carbon dioxide; **e**, methane flux; **f**,
638 nitrous oxide flux. Different letters and asterisk indicate significant difference between
639 groups by Wilcox sign test with p-value < 0.01.

640 **Figure 4. Changes in microbial diversity and structure in response to switchgrass**
641 **planting. a**, Number of observed species through time; **b**, Phylogenetic diversity. **c**,
642 Detrended correspondence analysis of the 16S community separated by site for all time
643 points and plots. Significant differences were found between sites, plant cover types, and
644 through time (PERMANOVA, p < 0.01). Dark colors represent the switchgrass samples.

645 **Figure 5. Changes of relative abundance for major phyla.** Taxonomic identity was
646 determined with the RDP classifier at 80% sequence match criteria. OTU table was
647 trimmed by abundant OTUs (> 0.001%). Difference between time points within each plot
648 for: **a**, Clay-loam switchgrass (CL-SG) plot; **b**, Clay-loam fallow (CL-FL) plot; Silt-loam
649 switchgrass (SL-SG) plot; Silt-loam fallow (SL-FL) plot. Significant differences between
650 the pervious time point for each group denoted by asterisk (*) symbols within each phyla
651 bar.

Figure 6. Relationships between environmental factors and microbial communities structure. Canonical correspondence analysis (CCA) linking microbial communities structure with environmental variables. Samples are shown by plot and site type with significant environmental variables shown in black arrows.

Figure 7. Structural equation modeling showing the relationships among environmental variables and GHG fluxes. a: Model for total carbon dioxide flux generated from the seasonal data (χ^2 = 25.806, d.f. = 18, P = 0.104, n = 588). **b**: Model for methane flux generated from seasonal data of switchgrass plots only (χ^2 = 10.116, d.f. = 9, P = 0.341, n = 294). Red and blue arrows represent significant ($p < 0.05$) positive and negative pathways, respectively. Numbers near the pathway arrows indicate the standard path coefficients (β). Width of the arrows are proportional to the strength of the relationship. Gray arrows represent residual correlations accounted for in the model. Plant Cover = Switchgrass (positive) or mixed annual grassland plant cover (negative) at the plot; Site = SL (positive) or CL (negative) soil site; CO_2 = total soil carbon dioxide flux; Soil Temp = soil temperature at a depth of 10 cm for bare soil in degrees Celsius; Soil Moisture = gravimetric per cent soil moisture; P = plant available phosphorus content; Microbial Alpha Diversity = number of observed bacterial species per sample; NO_3 = nitrate concentrations; CH_4 = methane flux; and pH = soil pH.

674

Table

Table 1: Differences in physico-chemical soil properties for each site and treatment after 17-months. Values are mean ± SD values and significance was tested by Kruskal-Wallis rank sum test.

Variable	Silt Loam Fallow	Silt Loam Switchgrass	Kruskal-Wallis Tests			Clay Loam Fallow	Clay Loam Switchgrass	Kruskal-Wallis Tests		
	Mean ± SD	Mean ± SD	Chi-squared	p	Effect Size	Mean ± SD	Mean ± SD	Chi-squared	p	Effect Size
pH	6.5 ± 0.67	6.7 ± 0.95	1.32	0.25	-	5.73 ± 0.44	5.85 ± 0.57	2.17	0.14	-
Soil Moisture (%)	7.1 ± 4.1	8.7 ± 6	3.27	0.07	-	10.4 ± 6.8	9.82 ± 5.5	0.75	0.39	-
Total soil C (%)	0.47 ± 0.09	0.61 ± 0.12	118	**< 0.0001*** **	0.40 Large	1.3 ± 0.42	1.3 ± 0.36	0.86	0.40	-
Total soil N (%)	0.06 ± 0.01	0.07 ± 0.01	55.4	**< 0.0001*** **	0.19 Medium	0.11 ± 0.02	0.11 ± 0.02	0.27	0.6	-
Phosphorus (ppm)	55.6 ± 13	73.7 ± 9.7	128	**< 0.0001 *** **	0.44 Large	22.6 ± 9.7	17.5 ± 6.5	27.7	**< 0.001****	0.095 Medium
Nitrate (ppm)	3.5 ± 3.7	2.2 ± 3	16.8	**< 0.001****	0.06 Small	8.3 ± 9.8	8.9 ± 15	2.37	0.12	-
Ammonium (ppm)	13.6 ± 11	14.5 ± 10	1.73	0.19	-	18.5 ± 11	17.9 ± 11.5	0.61	0.44	-

*Effect size shown by *epsilon* squared with small (0.01 - < 0.08), medium (0.08 - < 0.26), and large (≥ 0.26) ranges.

Figures

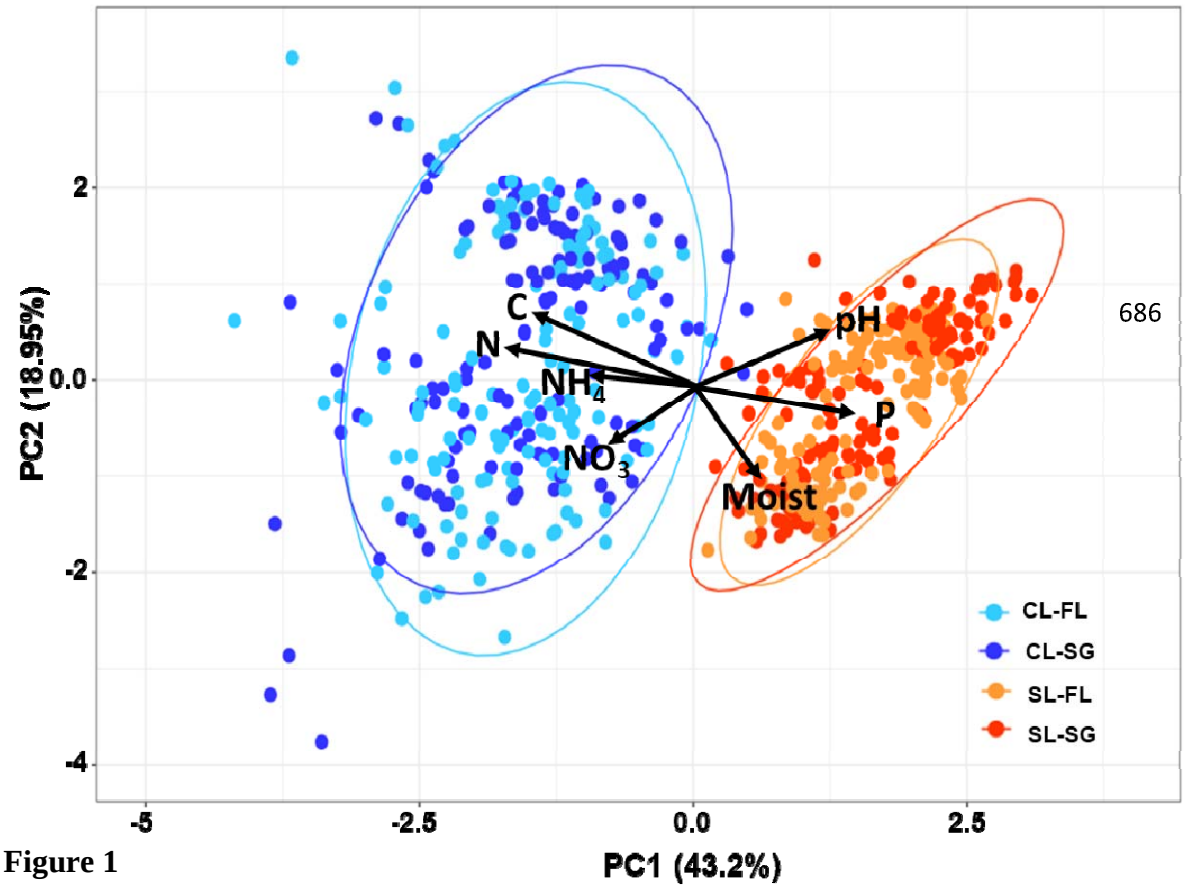

Figure 1

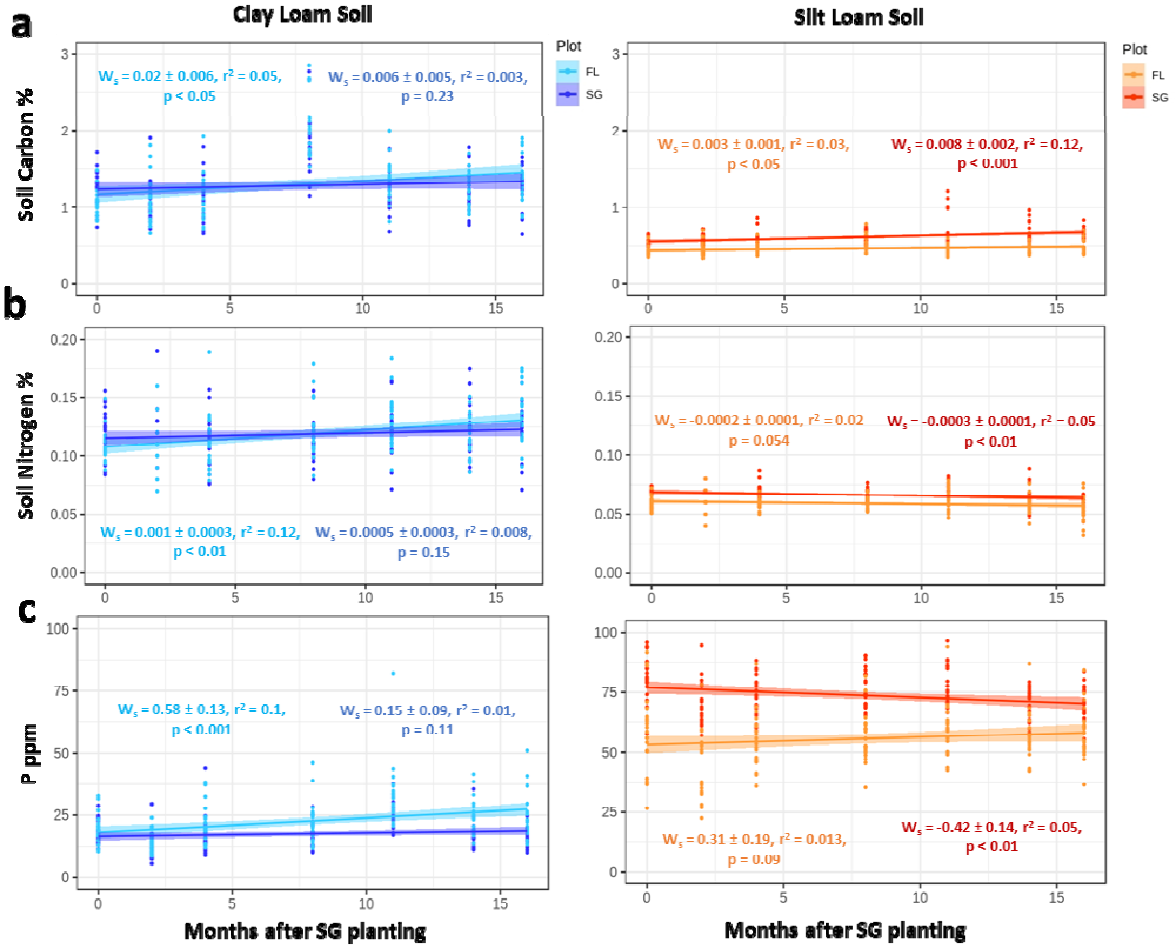

688

689 **Figure 2**

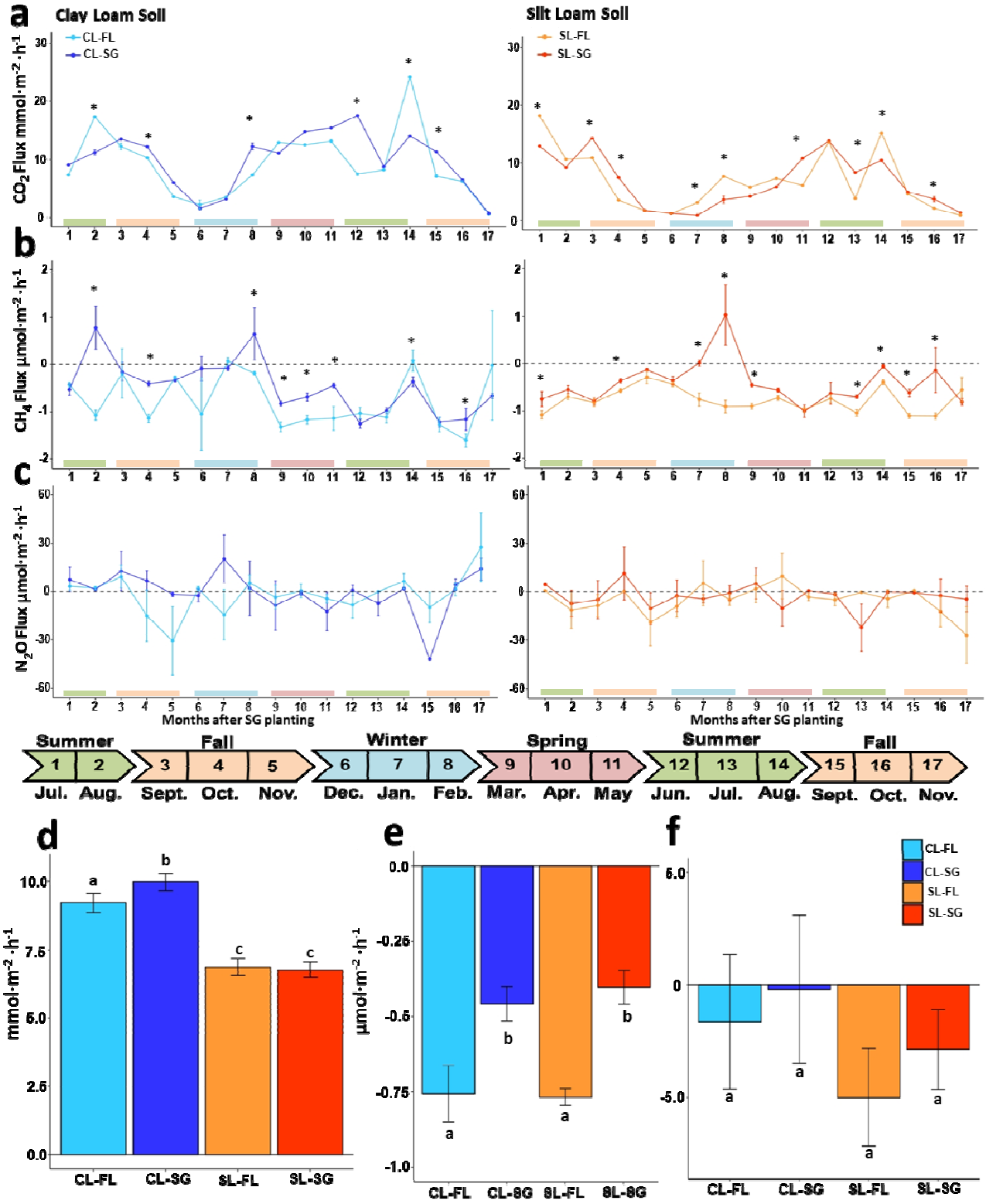

690

691 **Figure 3**

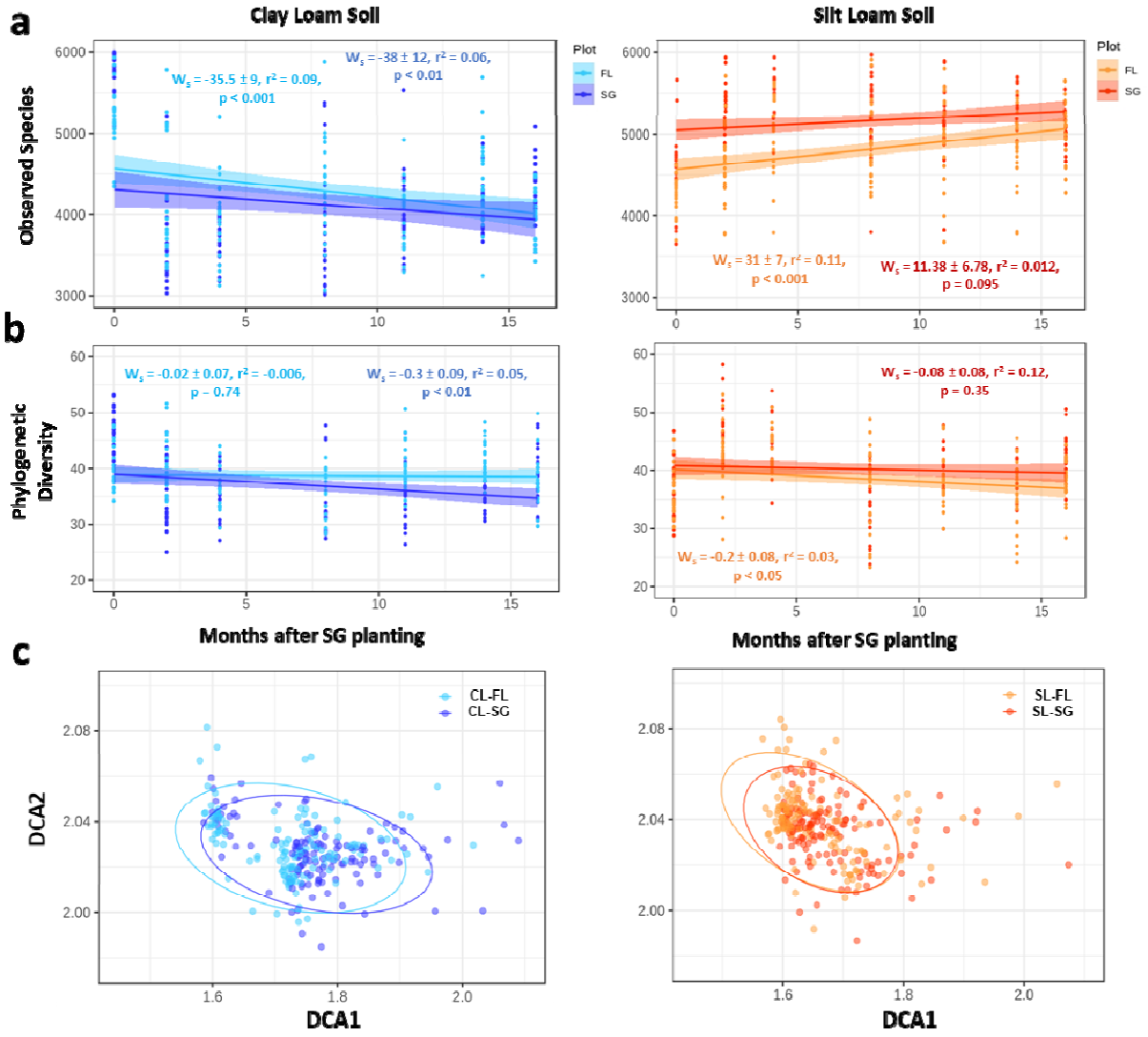

Figure 4

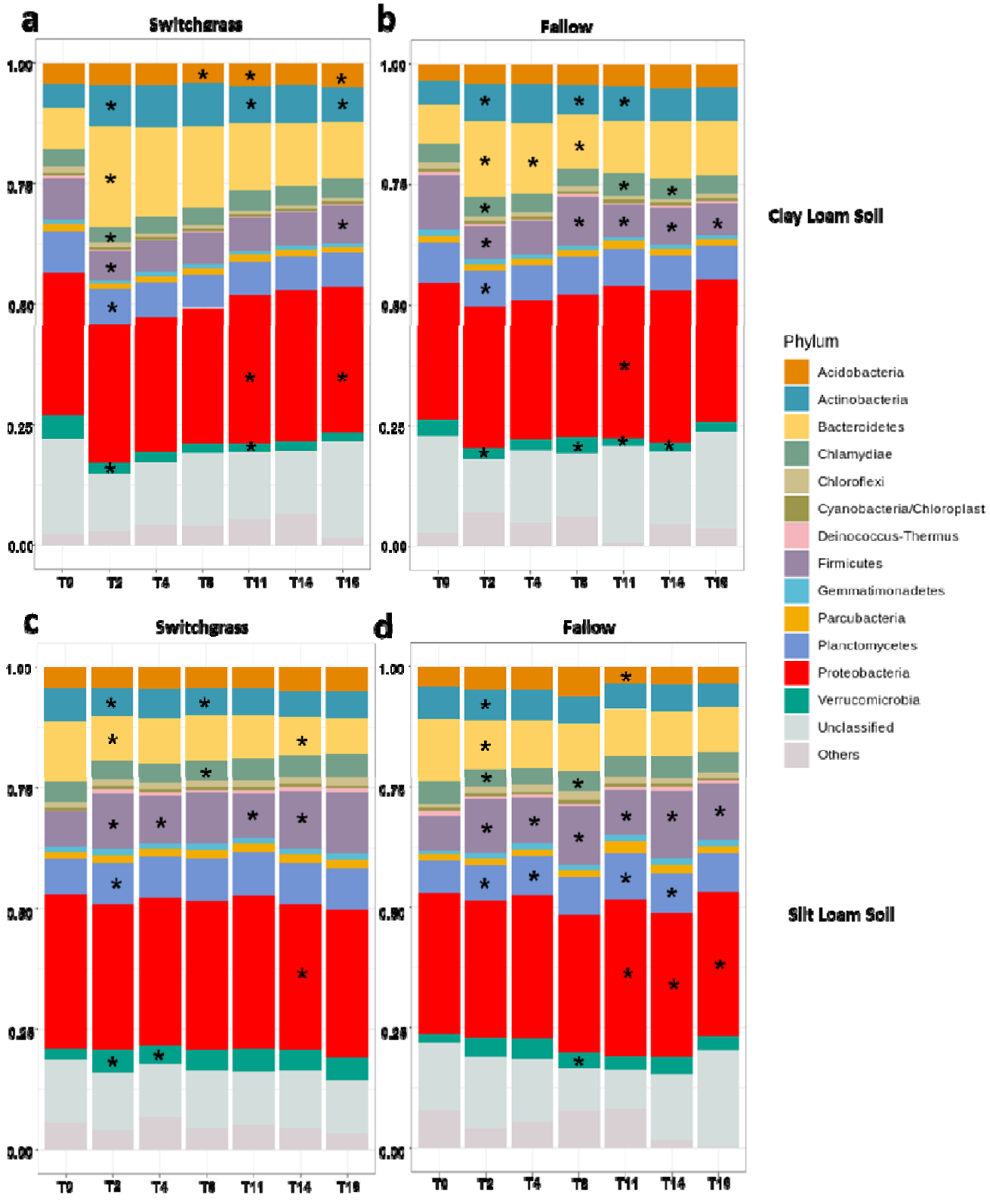

699

700 **Figure 5**

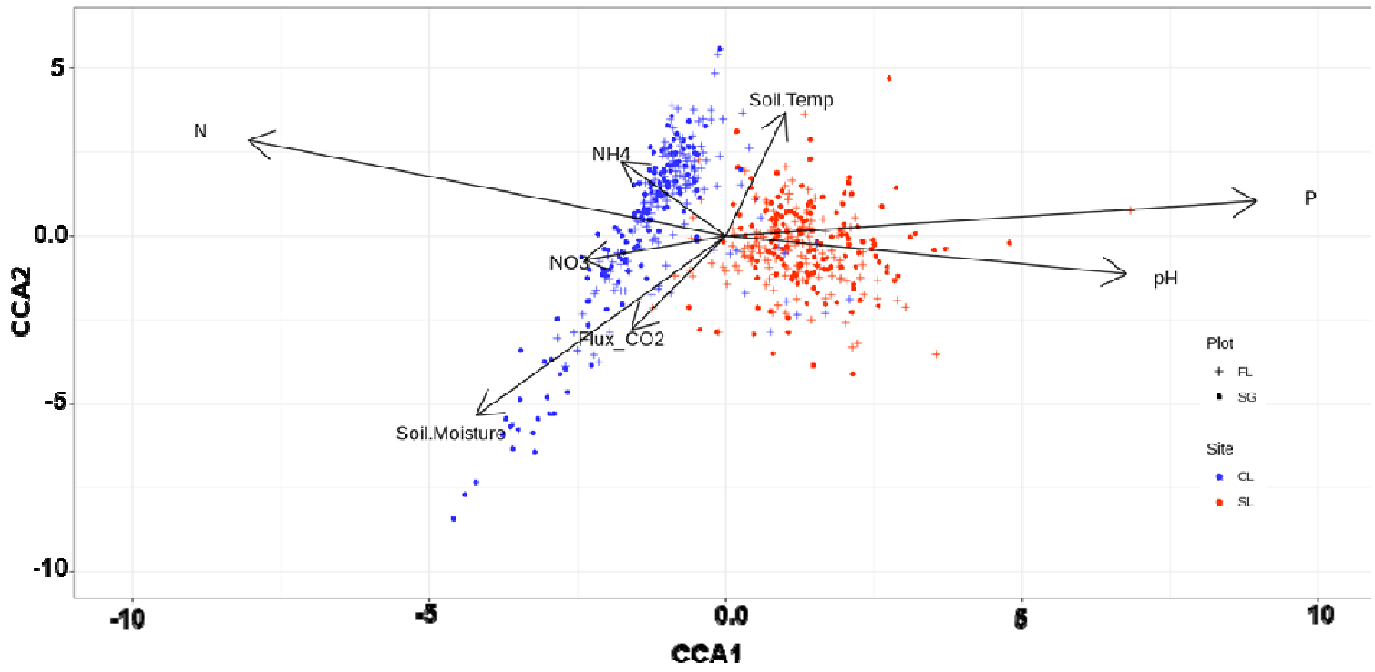

Figure 6

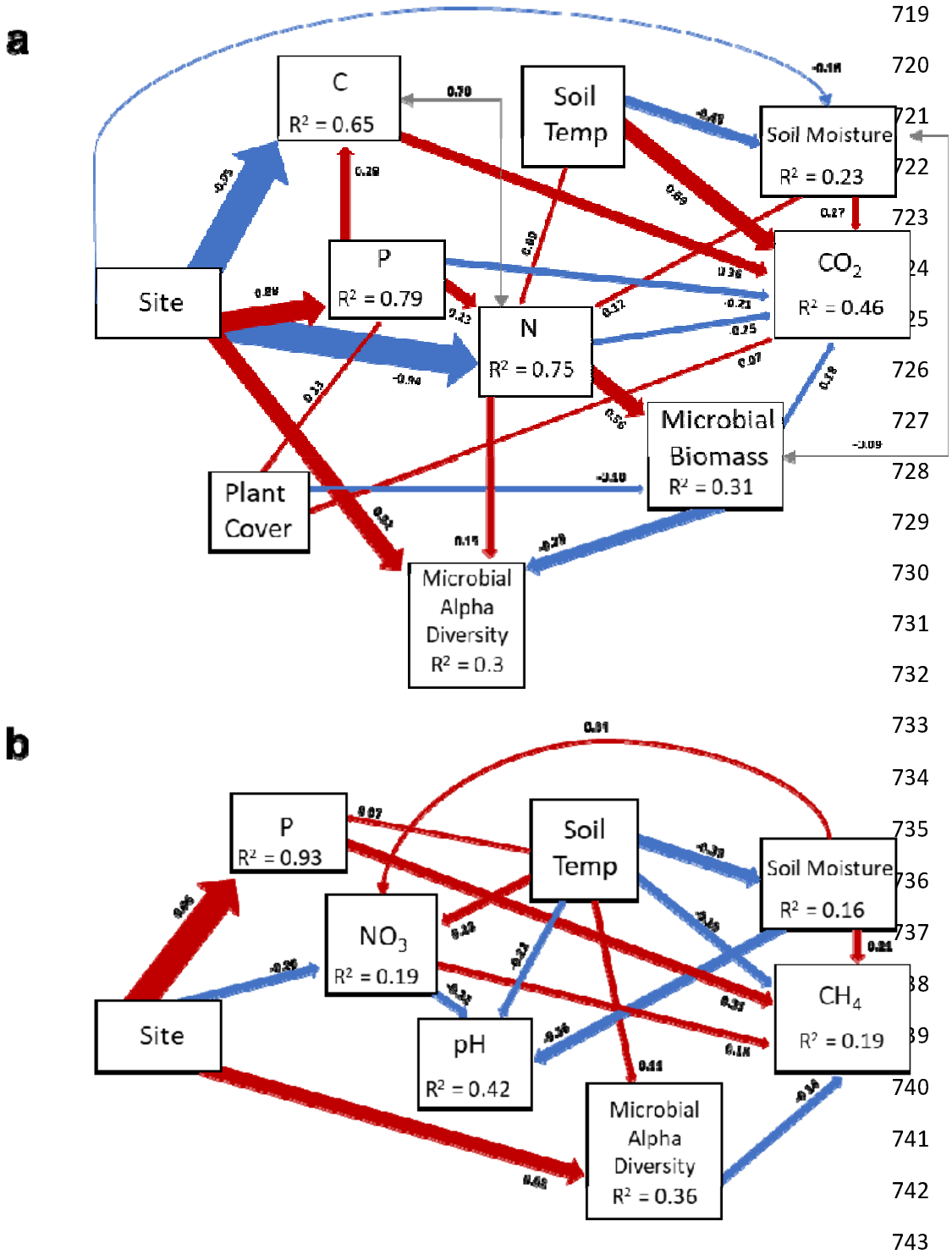

Figure 7

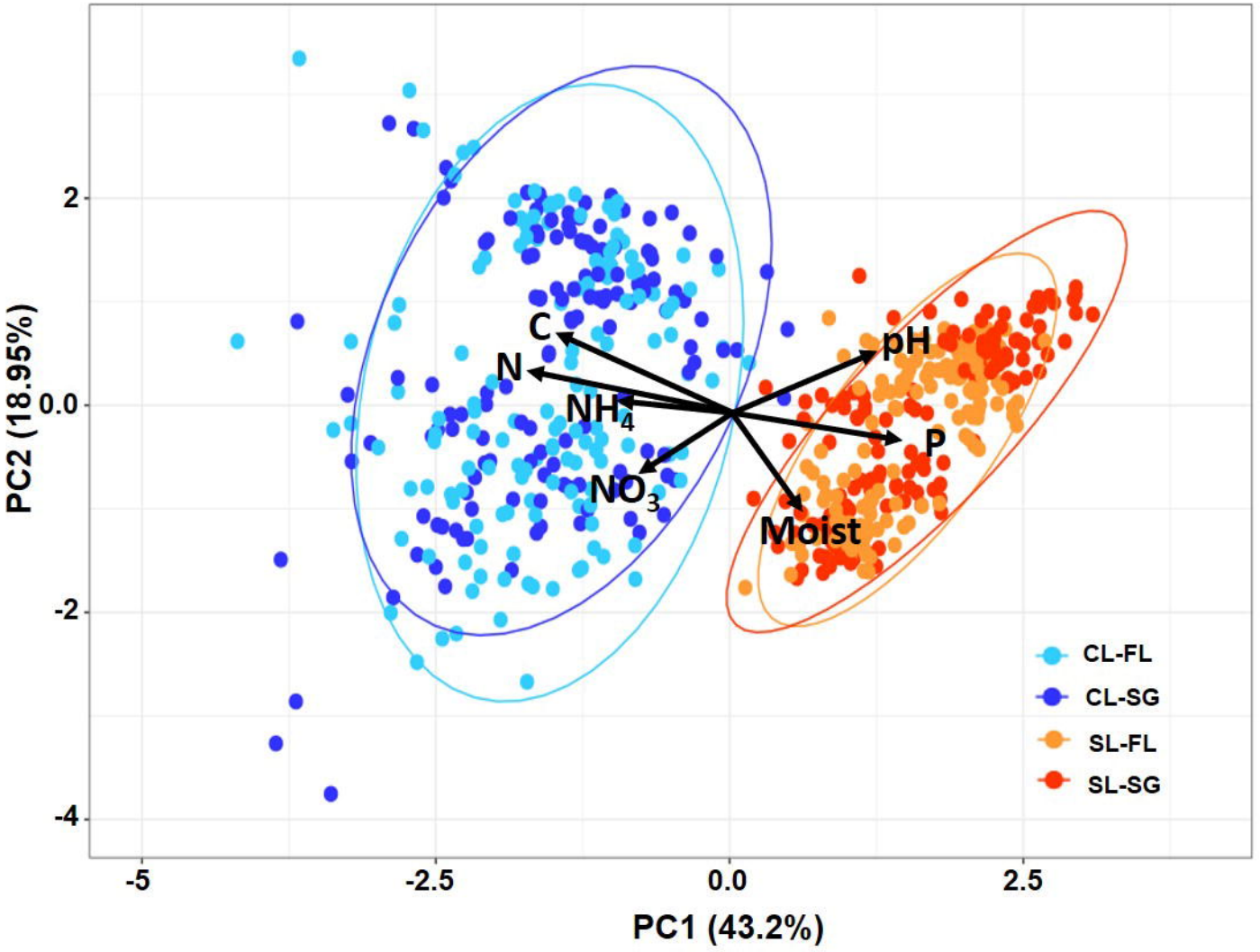

Figure 1. **Differences in soil geochemical properties between the two studied sites**. Principal component analysis. Blue colors represent the CL site while red/orange colors signify the SL site. Dark colors represent the SG samples. Variation contained in each PC axis are displayed next to each axis.

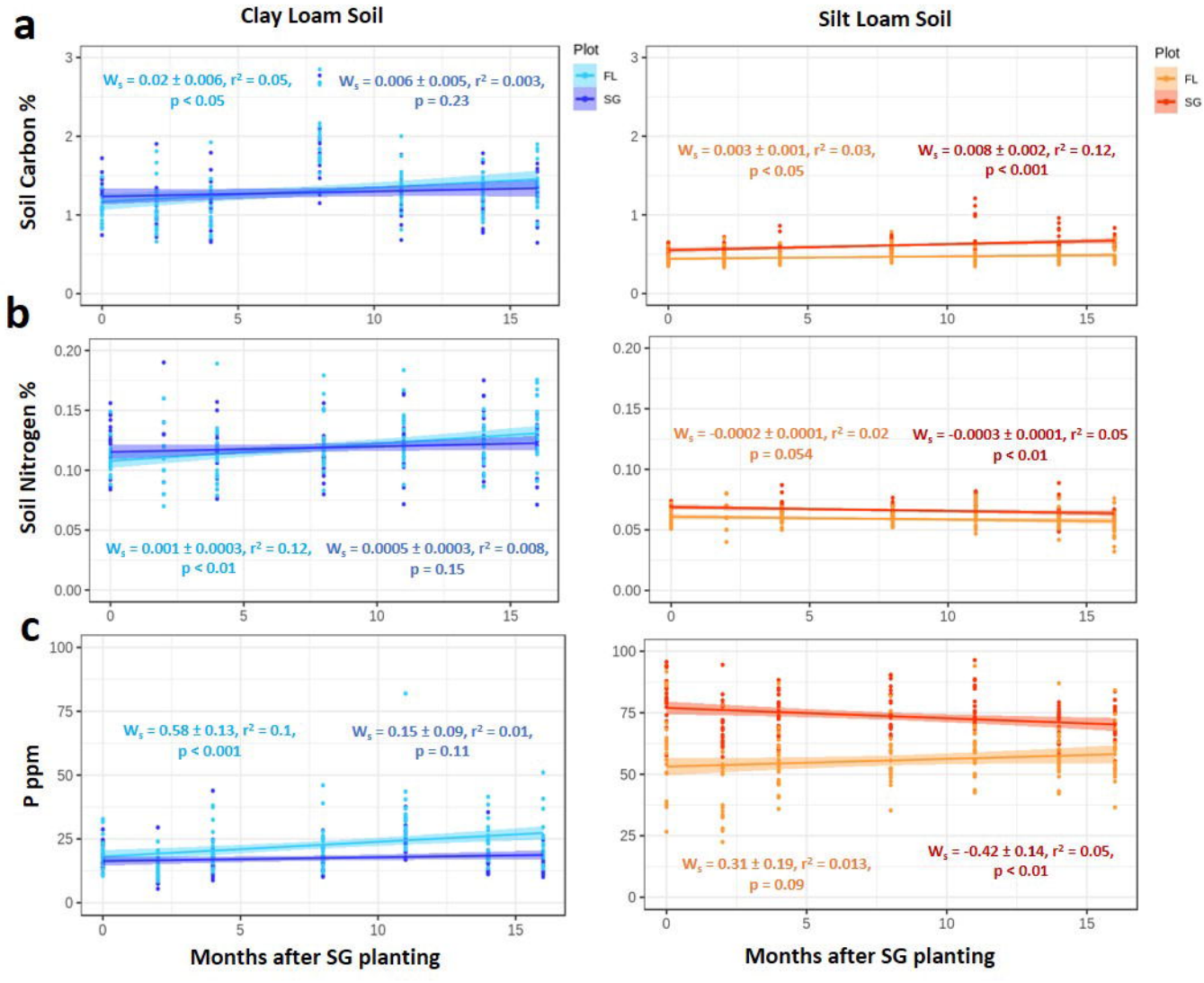

Figure 2. Changes in soil chemistry through two seasons of switchgrass establishment. **a**, Total soil carbon percentages; **b**, Total soil nitrogen percentages; **c**, Concentration of plant available phosphate content in parts per million. The best linear model describing the relationship is presented. W_S: estimated model slope and associated error. p-values represent the significance of each model. Each time point is comprised of twenty-one replicates per plot.

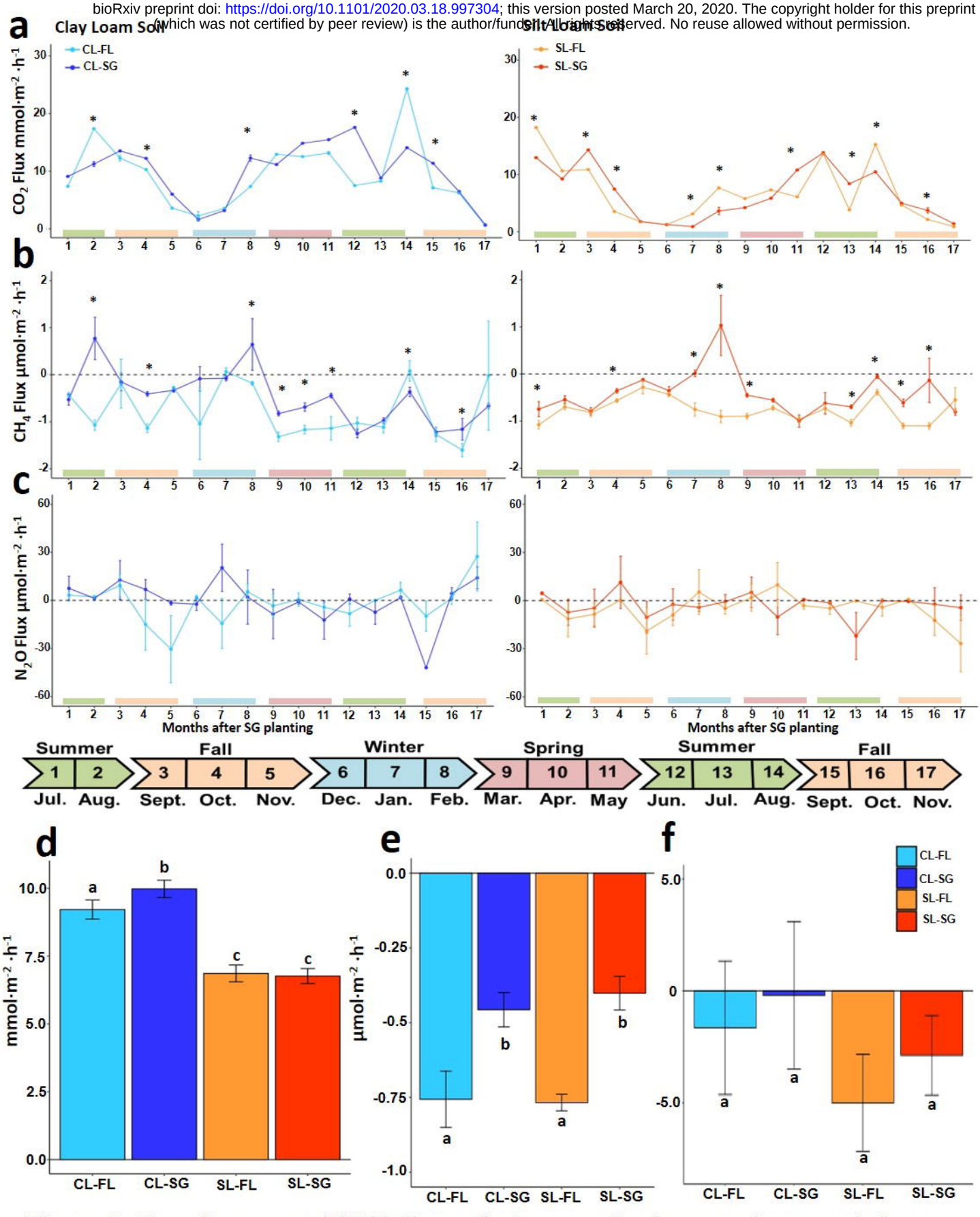

Figure 3. Greenhouse gas (GHG) fluxes during grassland conversion to switchgrass. **a**, **b**, **c**: GHG fluxes at each site over 17 months (mean and standard error estimated using 21 replicates for each time points) for: **a**, carbon dioxide flux; **b**, methane flux; **c**, nitrous oxide. **d**, Average GHG fluxes over 17-months for: **d**, carbon dioxide; **e**, methane flux; **f**, nitrous oxide flux. Different letters and asterisk indicate significant difference between groups by Wilcox sign test with p-value < 0.01.

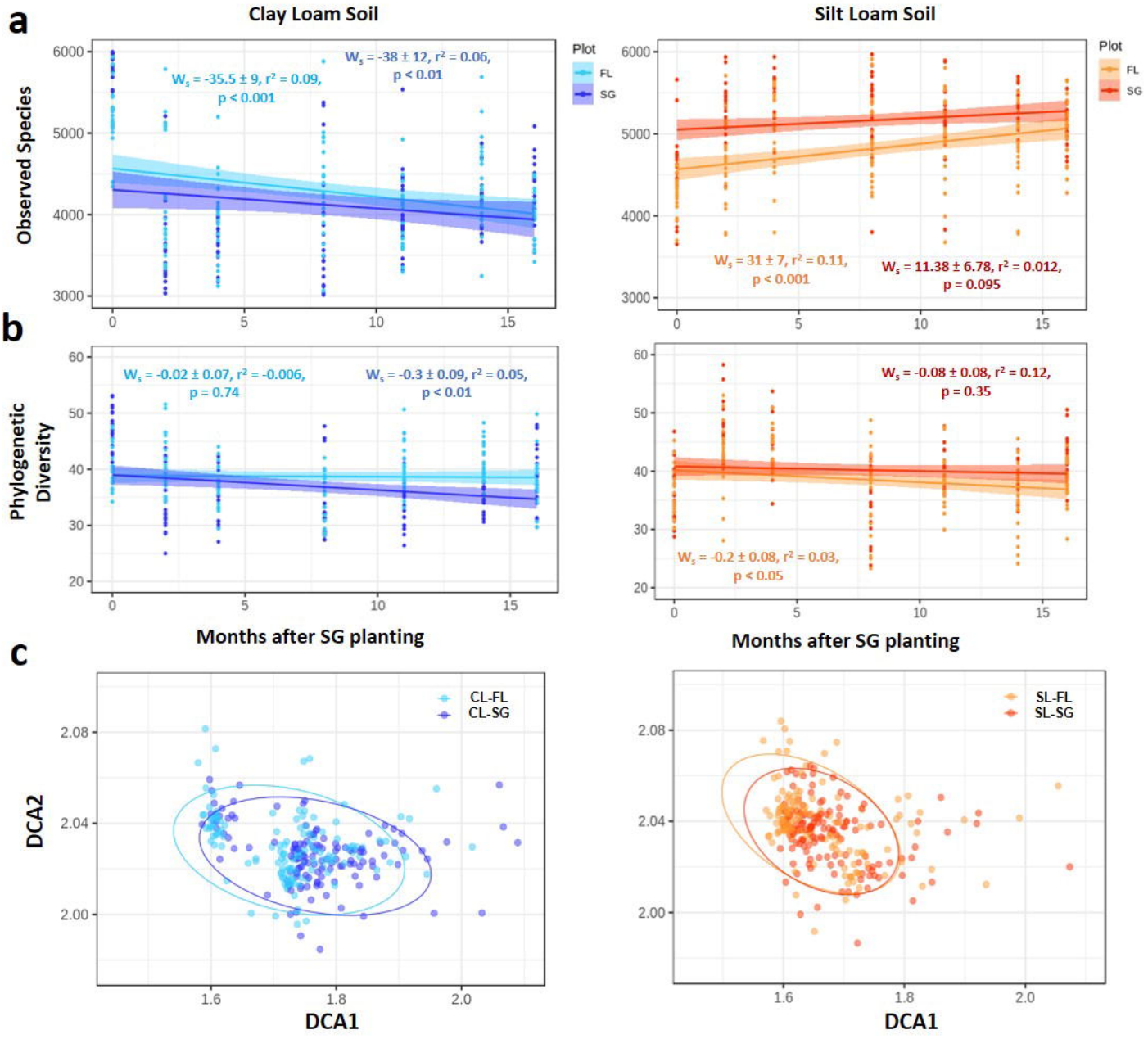

Figure 4. Changes in microbial diversity and structure in response to switchgrass planting. **a**, Number of observed species through time; **b**, Phylogenetic diversity. **c**, Detrended correspondence analysis of the 16S community separated by site for all time points and plots. Significant differences were found between sites, plant cover types, and through time (PERMANOVA, $p < 0.01$). Dark colors represent the switchgrass samples.

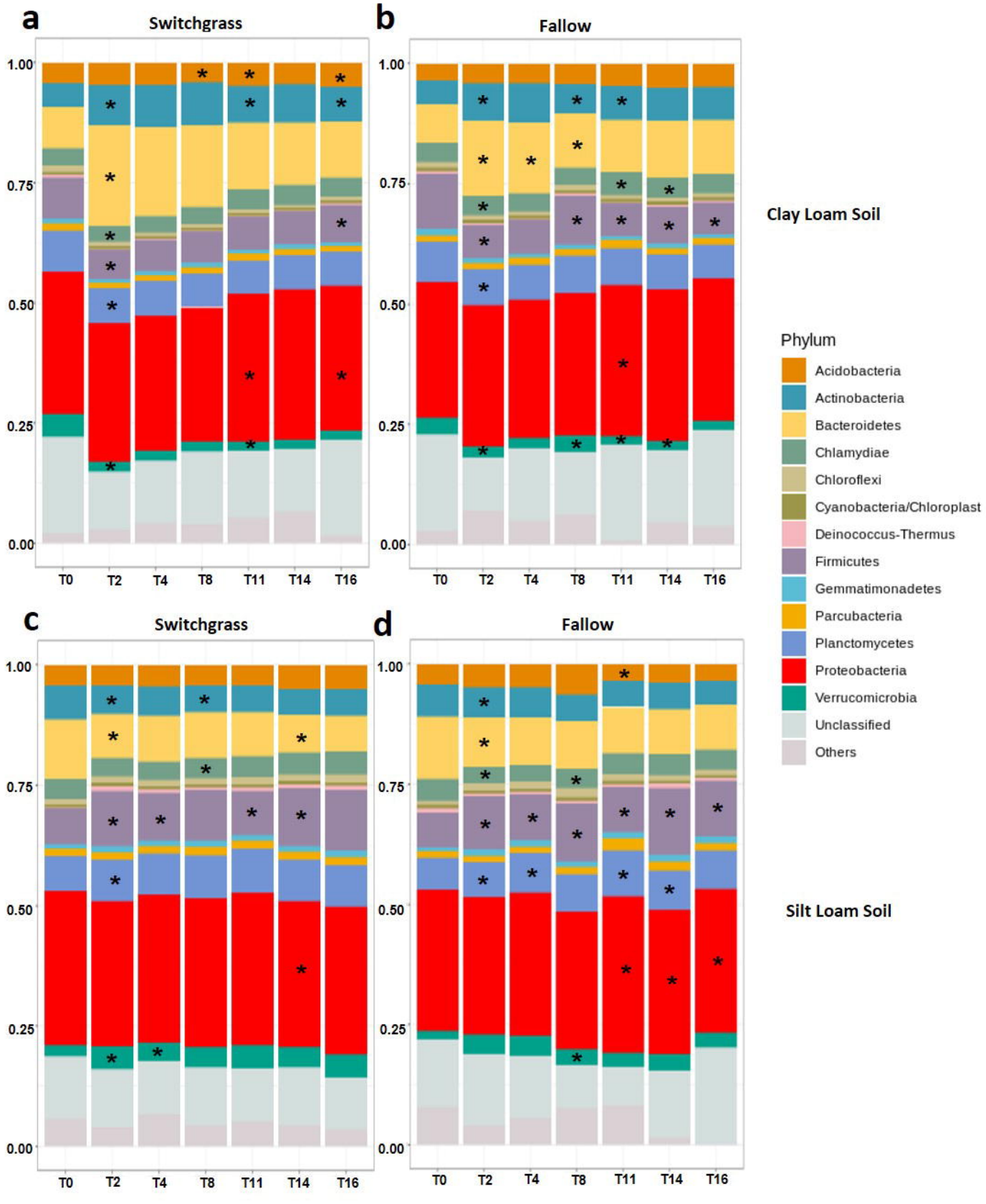

Figure 5. Changes of relative abundance for major phyla. Taxonomic identity was determined with the RDP classifier at 80% sequence match criteria. OTU table was trimmed by abundant OTUs (> 0.001%). Difference between time points within each plot for: **a**, Clay-loam switchgrass (CL-SG) plot; **b**, Clay-loam fallow (CL-FL) plot; Silt-loam switchgrass (SL-SG) plot; Silt-loam fallow (SL-FL) plot. Significant differences between the pervious time point for each group denoted by asterisk (*) symbols within each phyla bar.

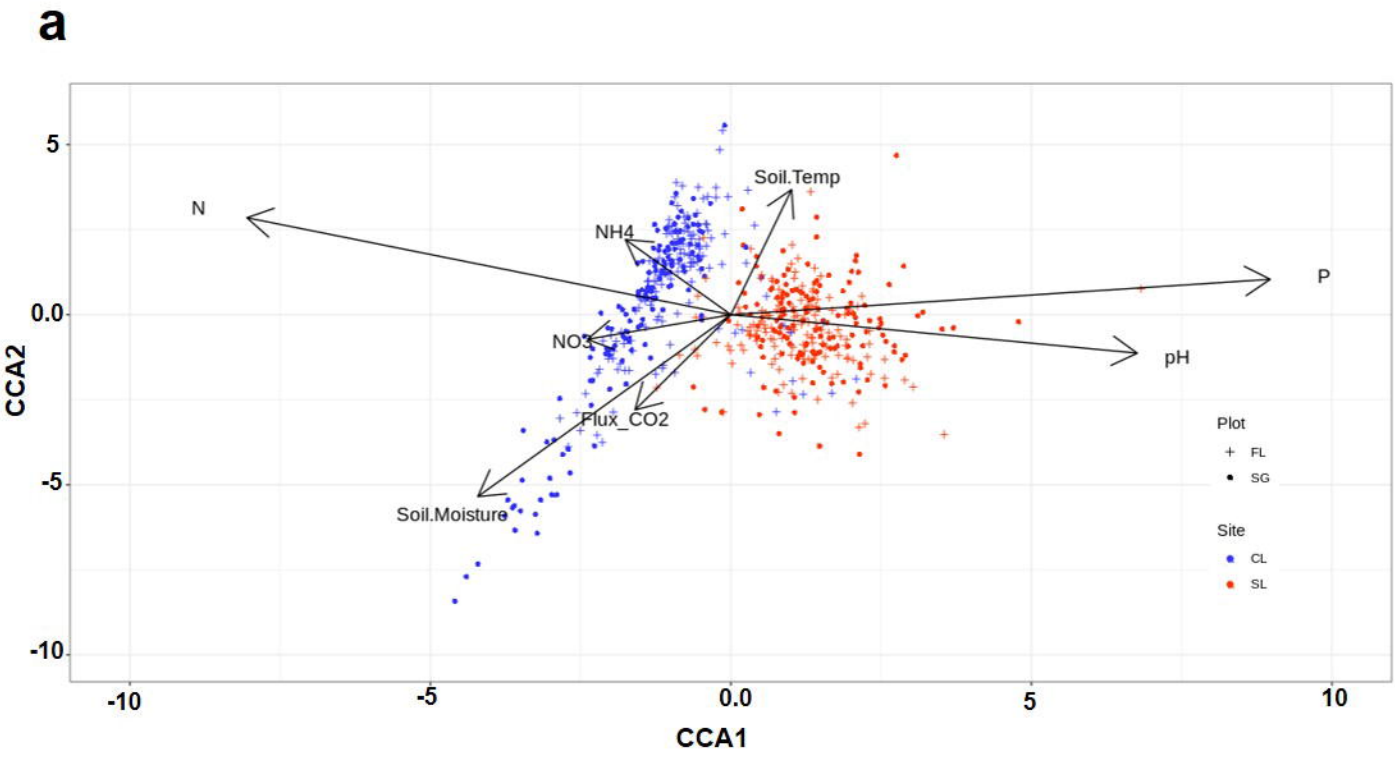

Figure 6. Relationships between environmental factors and microbial communities structure. Canonical correspondence analysis (CCA) linking microbial communities structure with environmental variables. Samples are shown by plot and site type with significant environmental variables shown in black arrows.

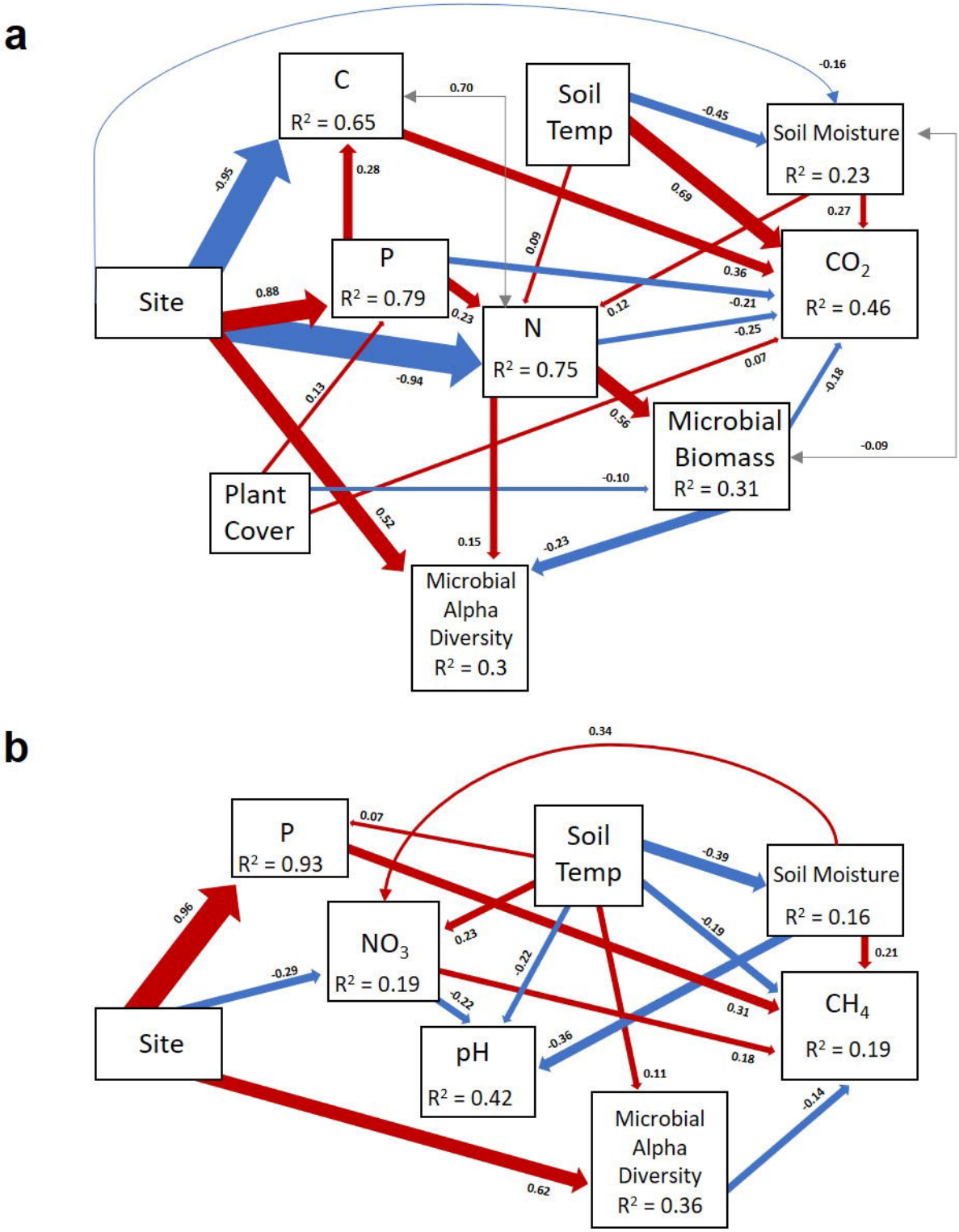

Figure 7. Structural equation modeling showing the relationships among environmental variables and GHG fluxes. a: Model for total carbon dioxide flux generated from the seasonal data ($\chi^2 = 25.806$, d.f. = 18, $P = 0.104$, $n = 588$). **b**: Model for methane flux generated from seasonal data of switchgrass plots only ($\chi^2 = 10.116$, d.f. = 9, $P = 0.341$, $n = 294$). Red and blue arrows represent significant ($p < 0.05$) positive and negative pathways, respectively. Numbers near the pathway arrows indicate the standard path coefficients (β). Width of the arrows are proportional to the strength of the relationship. Gray arrows represent residual correlations accounted for in the model. Plant Cover = Switchgrass (positive) or mixed annual grassland plant cover (negative) at the plot; Site = SL (positive) or CL (negative) soil site; CO_2 = total soil carbon dioxide flux; Soil Temp = soil temperature at a depth of 10 cm for bare soil in degrees Celsius; Soil Moisture = gravimetric per cent soil moisture; P = plant available phosphorus content; Microbial Alpha Diversity = number of observed bacterial species per sample; NO_3 = nitrate concentrations; CH_4 = methane flux; and pH = soil pH.

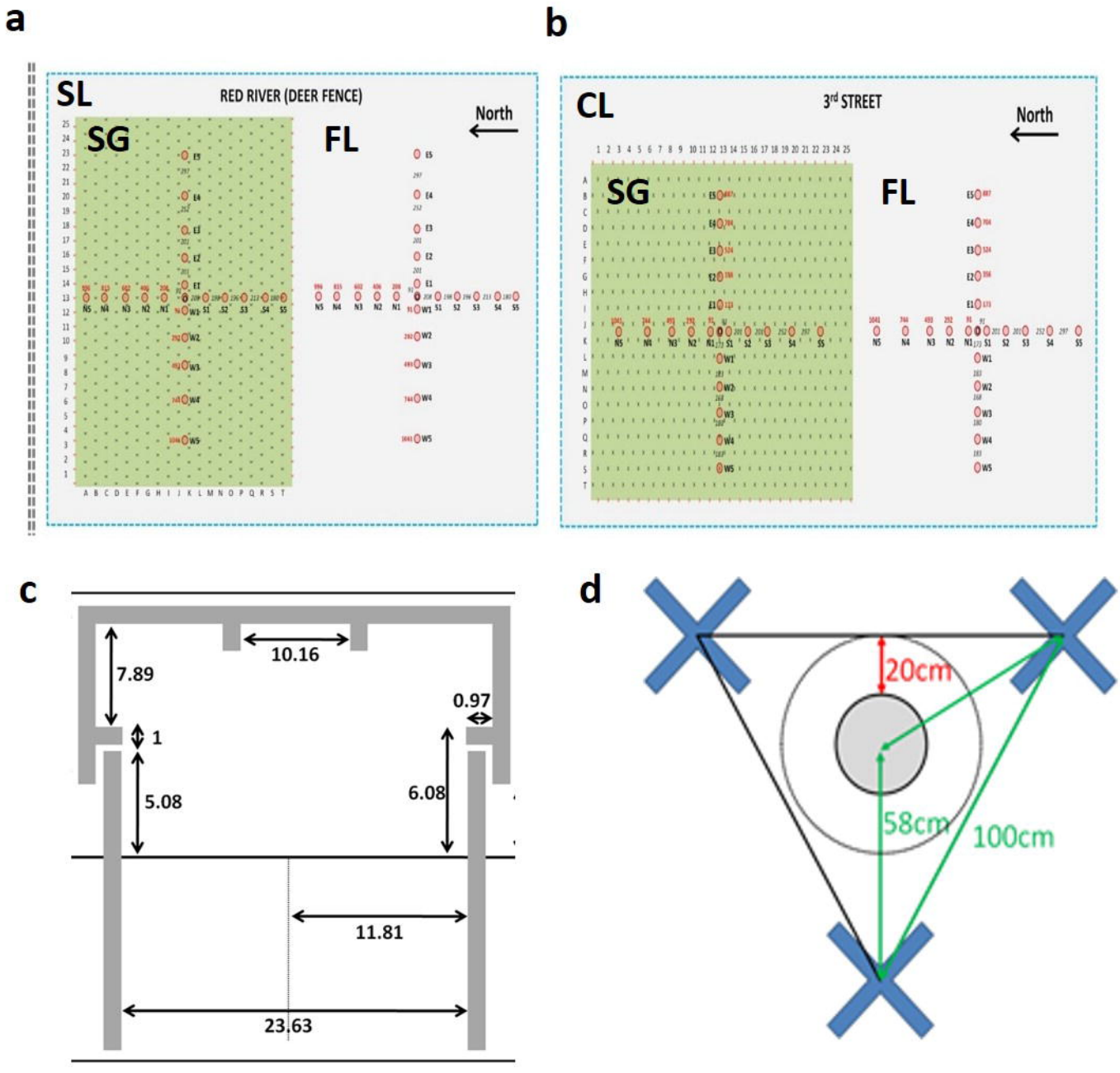

Fig. S1, Layout for the field sites, collar positions, and soil sampling details: a, layout of the SL field site and location of trace gas collars for each plot; **b**, layout of the CL field site and location of the trace gas collars for each plot; **c**, diagram of trace gas collar and chamber dimensions; **d**, diagram of collar position in relation to switchgrass plants and soil sampling details. Blue X's represent switchgrass plants and the gray circle represents the trace gas collar.

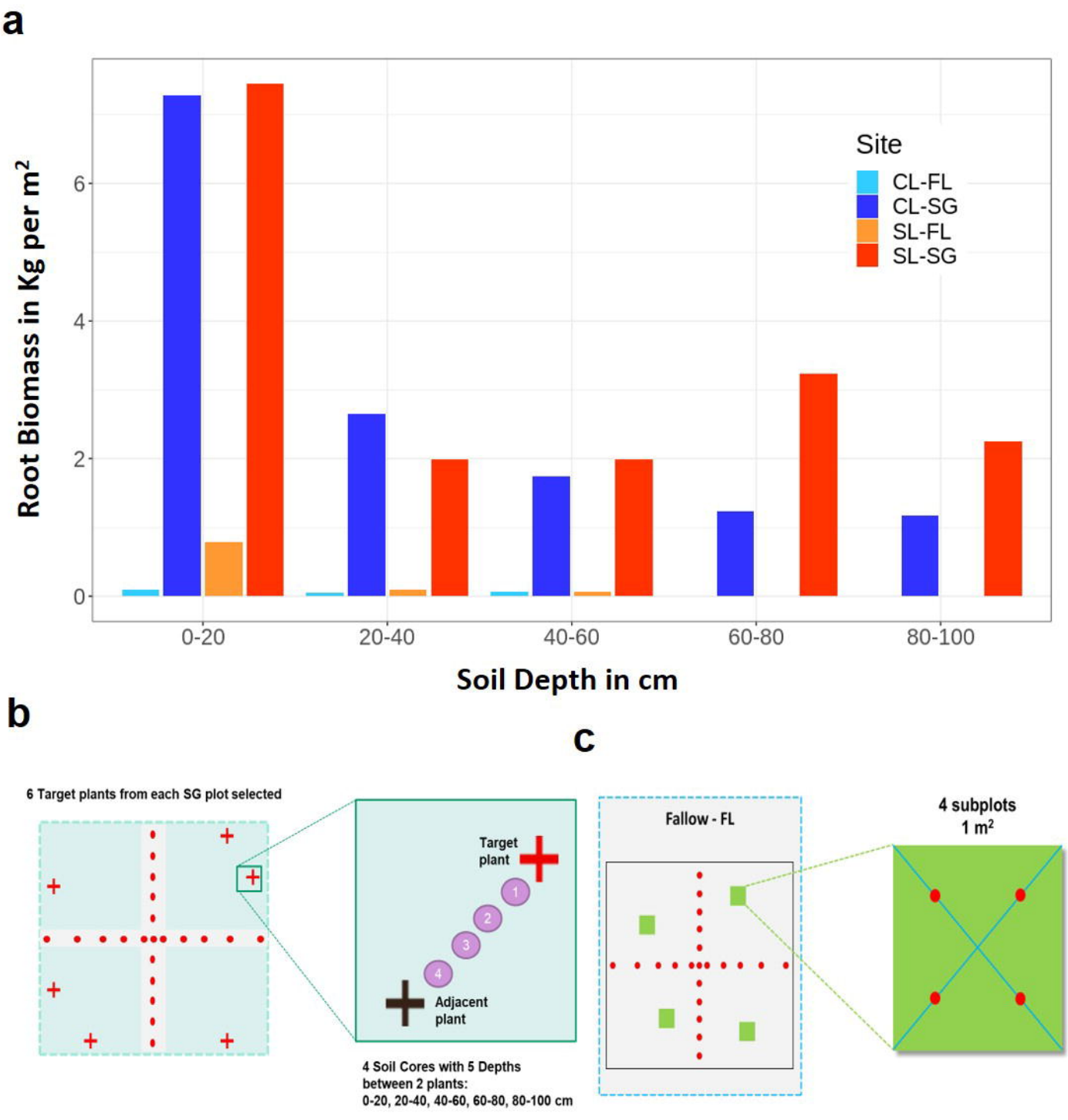

Fig. S2, Root biomass estimates and methods for: a, difference between fallow and switchgrass plots for estimated root biomass by depths; **b**, graphic for how switchgrass plants were selected for root biomass estimation; **c**, graphic for how fallow root biomass estimation was conducted using four 1 m^2 subplots in each quadrant of the plot.

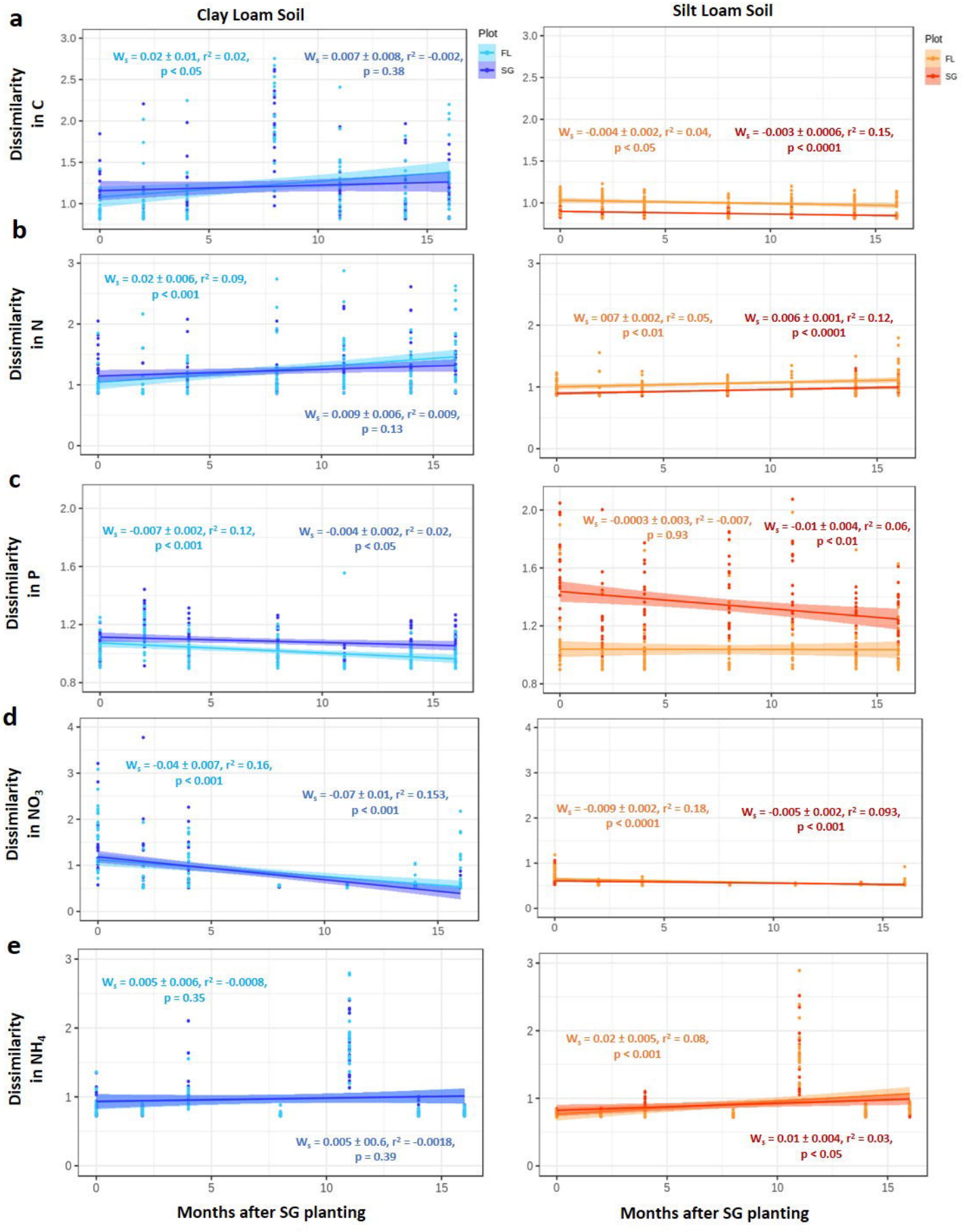

Fig. S3, Dissimilarity between soil chemistry samples through the seasons at each site between SG and FL plots for: a, dissimilarity in soil carbon samples; **b**, dissimilarity in soil nitrogen content; **c**, dissimilarity in plant available phosphate content; **d**, dissimilarity in nitrate content; **e**, dissimilarity in ammonium. Ws is the slope of each line and the error associated with each slope while p-values represent the significance of each trend line. Each time point is comprised of twenty-one replicates per plot.

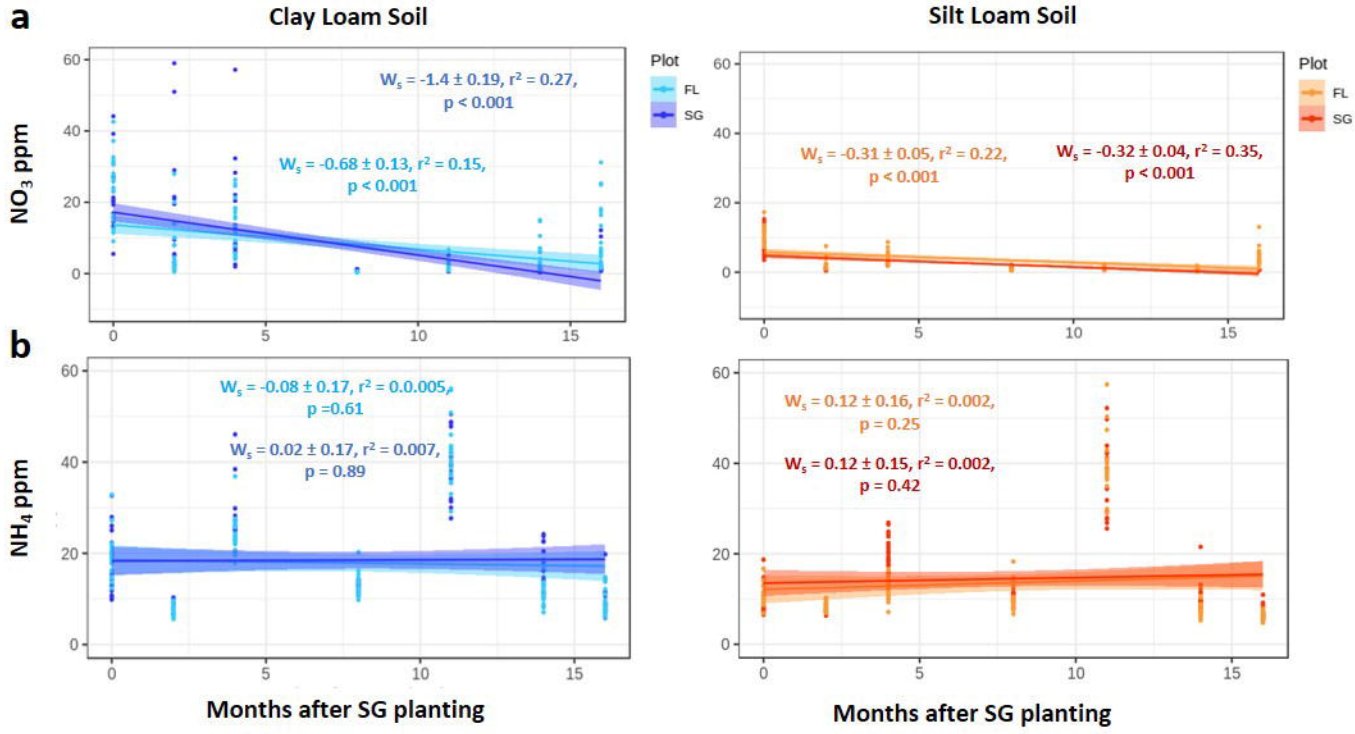

Fig. S4, Changes in soil chemistry through the seasons at each site between SG and FL plots for: a, concentration of nitrate content; **b**, ammonium content. Ws is the slope of each line and the error associated with each slope while p-values represent the significance of each trend line. Each time point is comprised of twenty-one replicates per plot.

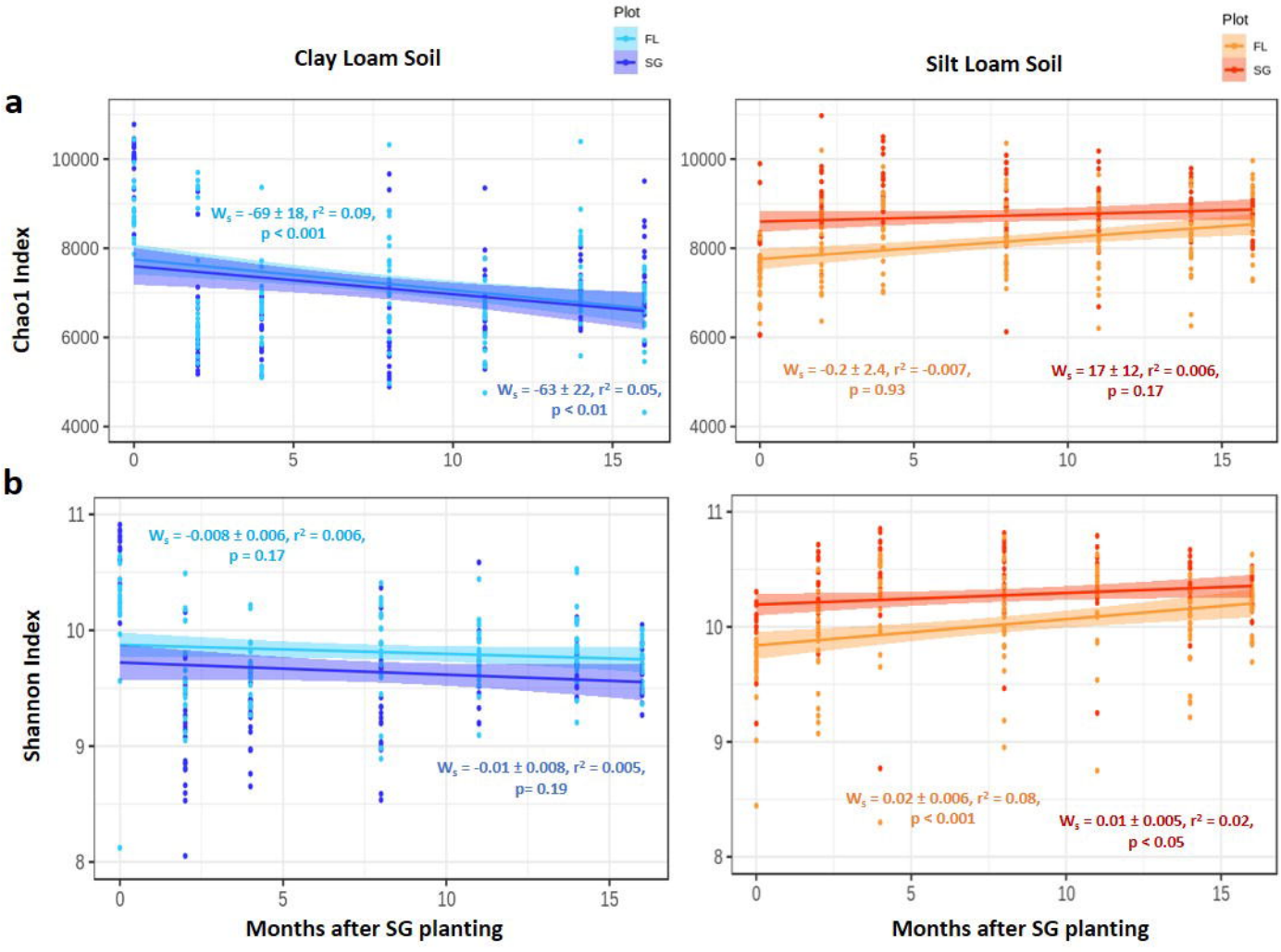

Fig. S5, Change in microbial alpha diversity measures through the seasons at each site between SG and FL plots for: a, chao1 index; **b**, Shannon index. Ws is the slope of each line and the error associated with each slope while p-values represent the significance of each trend line. Each time point is comprised of twenty-one replicates per plot.

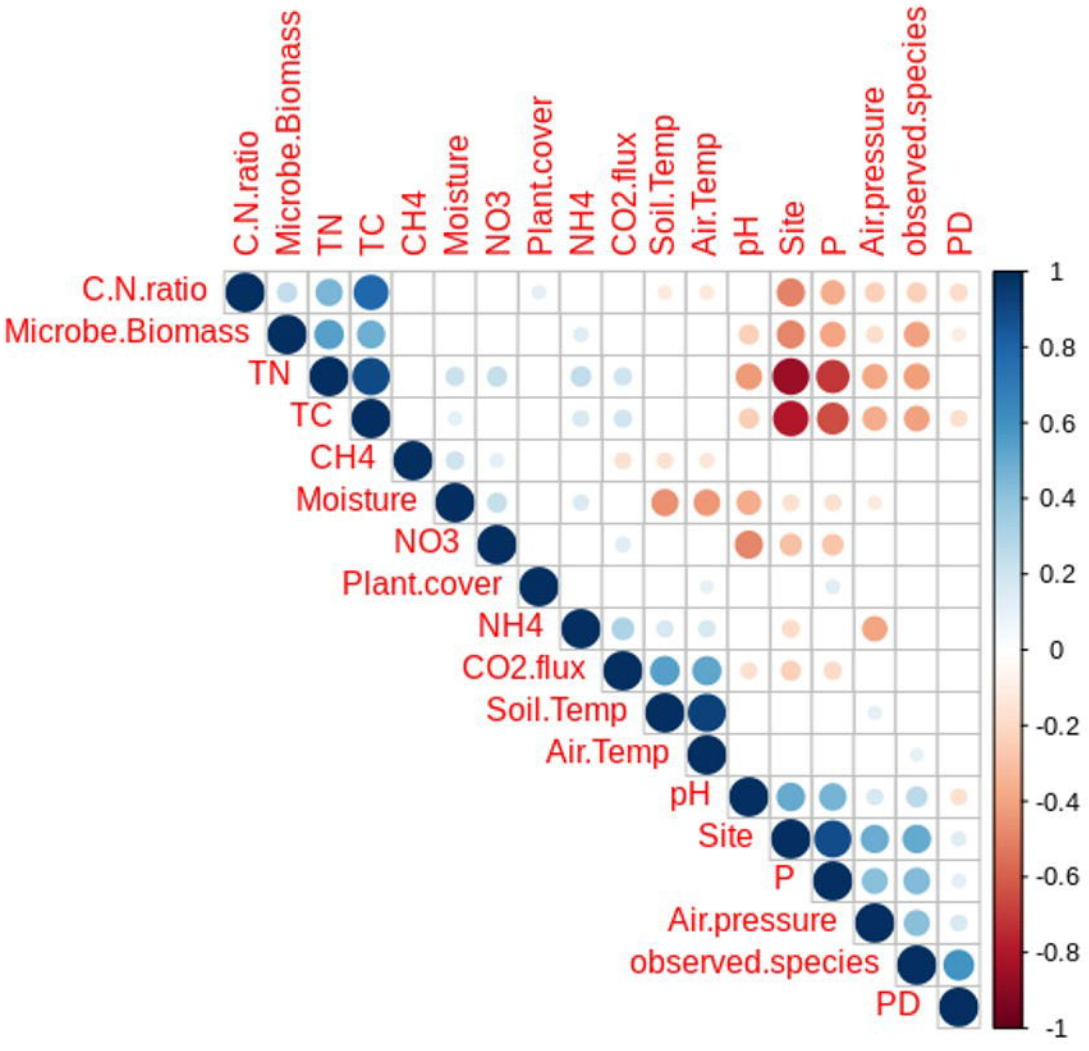

Fig. S6, Correlation plot between environmental, microbial, and soil geochemistry variables. Blue circles indicate significant positive correlations while red circles indicate negative correlations. Larger darker circles indicate a more significant and stronger correlation between variables. Positive correlations for site represent SL site while negative correspond to the CL site. 'Microbe.Biomass' was estimated using DNA concentrations after soil extractions. 'observed.species' is the total species richness (alpha diversity) of the samples. 'PD' represents the whole tree phylogenetic diversity of the plots. Positive correlations for 'Plant.cover' represent switchgrass plots and negative for fallow plots.